ERDC/CERL TR-01-36

US Army Corps of Engineers®
Engineer Research and Development Center

Historical Analysis of Land Cover/Condition Trends at Fort Bliss, Texas, Using Remotely Sensed Imagery

Scott A. Tweddale

April 2001

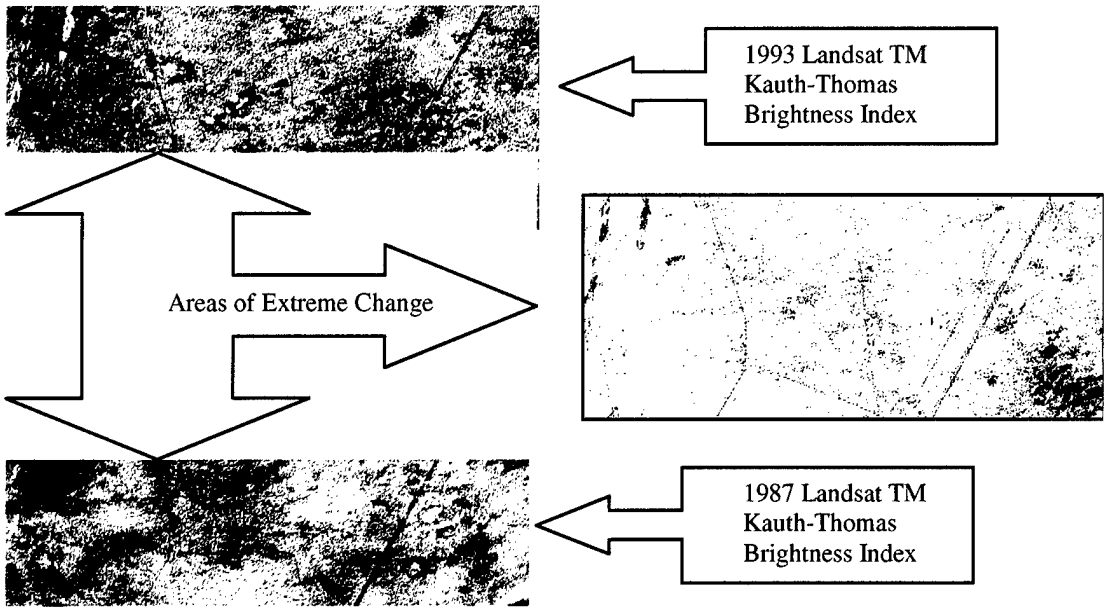

Construction Engineering Research Laboratory

Approved for public release; distribution is unlimited.

20010802 032

Foreword

This study was conducted for Commander, Directorate of Environment, Fort Bliss, Texas, under Military Interdepartmental Purchase Request (MIPR) #96-08; "Installation Vegetation Mapping." The technical monitors were Mr. Keith Landreth, Chief, Cultural and Natural Resources, and Mr. Kevin von Finger, NEPA Ecologist.

The work was performed by the Ecological Processes Branch (CN-N) of the Installations Division (CN), Construction Engineering Research Laboratory (CERL). The Principal Investigator was Mr. Scott Tweddale. The technical editor was Gloria J. Wienke, Information Technology Laboratory. Mr. Stephen E. Hodapp is Chief, CEERD-CN-N, and Dr. John T. Bandy is Chief, CEERD-CN. The associated Technical Director was Dr. William D. Severinghaus, CEERD-CV-T. The Acting Director of CERL is Dr. William D. Goran.

The author acknowledges Mr. Brett Russell, Mr. Dallas Bash, Mr. Kevin von Finger, and Mr. Rich Manning, Fort Bliss Directorate of Environment, for their assistance with field data collection.

CERL is an element of the U.S. Army Engineer Research and Development Center (ERDC), U.S. Army Corps of Engineers. The Director of ERDC is Dr. James R. Houston and the Commander is COL James S. Weller.

DISCLAIMER

The contents of this report are not to be used for advertising, publication, or promotional purposes. Citation of trade names does not constitute an official endorsement or approval of the use of such commercial products. All product names and trademarks cited are the property of their respective owners.

The findings of this report are not to be construed as an official Department of the Army position unless so designated by other authorized documents.

DESTROY THIS REPORT WHEN IT IS NO LONGER NEEDED. DO NOT RETURN IT TO THE ORIGINATOR.

Contents

List of Figures and Tables

Figures

Tables

1 Introduction

Background

A large number of U.S. Army training and testing installations are located in arid and semi-arid environments in the desert Southwestern United States. Fort Bliss, Texas, is a Training and Doctrine Command (TRADOC) installation located in the Northern Chihuahuan Desert of Western Texas and South Central New Mexico. At 1.1 million acres, it represents the single largest TRADOC installation. Fort Bliss exists within a semi-arid ecosystem; therefore it is highly susceptible to disturbance caused by both natural and anthropogenic factors. Disturbance in arid landscapes is usually associated with a decrease in vegetative cover and an increase in soil erosion, and can occur at many different scales. Military training (both tracked and wheeled), grazing, and recreational activities all act as stressors on the landscape at Fort Bliss. The Fort Bliss Directorate of Environment (DOE) is responsible for sustainment of natural resources in support of the training mission. Therefore, Fort Bliss natural resource managers require information on land condition to make informed land management decisions and to support conservation and compliance efforts, including direct support of Environmental Impact Statements (EISs) for withdrawal of Bureau of Land Management (BLM) lands for training. Fort Bliss natural resource managers require a cost-effective method for assessing and monitoring land condition.

Vegetation amount, condition, and composition are the most important indicators of land condition in arid environments; therefore, it is necessary to conduct inventories and monitor vegetation amount and condition (Robinove et al. 1981; Musick 1984; Duncan et al. 1993). Many Department of Defense (DOD) installations have implemented the Land Condition Trend Analysis (LCTA) program, which is part of the Integrated Training Area Management (ITAM) plan for the U.S. Army. LCTA provides a standard method of inventory and monitoring for vegetation and wildlife (Tazik et al. 1992). Permanent plots are established and visited annually to conduct a detailed census of vegetation and wildlife. However, field surveys are expensive; therefore, a complete survey of large installations is cost prohibitive and a detailed vegetation map is often lacking. Long-term trends in vegetation condition can be monitored by LCTA field surveys, but

it is not feasible to assess vegetation condition at any one time over a large area like Fort Bliss based solely on field surveys.

Remotely sensed imagery, because of its large areal coverage and high temporal frequency, provides an ideal supplement to field surveys when attempting to characterize and monitor changes in vegetation condition at different scales and levels of detail. Archival coarse resolution imagery can be used to detect *relative* changes in surface condition or vegetation cover in both small and large areas. Vegetation indices and soil brightness indices calculated from remotely sensed reflectance data are sensitive to the amount of vegetation on the Earth's surface. Special indices have been customized to address unique problems associated with reflectance characteristics of arid environments where vegetation cover typically is low. Assessing trends in vegetation and brightness indices calculated from temporal image data sets provides a cost-effective method for monitoring relative trends in land condition. Quantification of land condition with remotely sensed imagery is difficult and requires an empirical relationship between indices and ground measurements for the purpose of calibration. Historical ground surveys are not always available. However, documentation of historical trends in land condition is useful to upper management for evaluating the effectiveness of historical resource management efforts, including Land Rehabilitation and Maintenance (LRAM) over long periods of time and across large geographic areas. Documentation is also useful for generating support for continued efforts or identifying other "problem" areas where future resource management efforts should be focused. Detecting coarse resolution changes may provide general measures of significant change in percent cover for a training area or group of training areas, for example, but may not be able to detect more subtle changes in grass vs. shrub cover.

Objective

The objective of this research was to characterize the small scale, gross level change in land condition over 23 years for a selected area of Fort Bliss, Texas, based upon evaluation and analysis of several vegetation and brightness indices calculated from temporal, archival multispectral imagery.

Approach

A study area was defined to include most of Maneuver Areas 5C, 5D, and parts of 4B and 4C on the west side of U.S. Route 54 and an adjoining area extending approximately 4 to 5 kilometers (km) east across Route 54 onto the McGregor

Guided Missile Range. The study area represents a gradient of impact and was selected in consultation with the Fort Bliss Directorate of Environment (Mr. Kevin von Finger). The maneuver areas have been impacted to varying degrees during the time period of this study, while the area extending onto the McGregor Range has been relatively unimpacted by tracked and wheeled maneuvers during this same time period. An archival imagery set was acquired, georeferenced, and subsetted to the study site. Several vegetation and brightness indices were reviewed for their applicability in monitoring land condition in arid environments. Based on a literature survey, Red Reflectance, Modified Soil-Adjusted Vegetation Index (MSAVI2), Albedo, and the Tasseled Cap Brightness Index were selected for analysis and calculated for 19 image dates over a 23-year period. Trends in these indices were evaluated for heavily impacted maneuver areas, low impact areas, and the entire study site. These trends were used as surrogate measures of vegetation cover and land condition for this 23-year period to characterize relative changes that may have occurred.

Scope

The specific indices and resulting trends analyzed in this report are specific to Fort Bliss, Texas. However, assessment of relative trends in land condition based on vegetation and brightness indices calculated from temporal, multispectral imagery is a valid and cost-effective technique that should be applicable to many, but not all military installations. These techniques work best in environments with a relatively open canopy. In forested ecosystems, vegetation indices may provide some measure of land condition based on reflectance of the upper most strata of vegetation or forest canopy, but would not be sensitive to understory vegetation or vegetative ground cover if the canopy cover exceeds a certain density. The temporal period of 23 years (1972 through 1994) in this study represents nearly the maximum amount of time for which civilian satellite imagery has been available. Archival imagery of the same spatial and spectral resolution should be available for most DoD training and testing installations. Therefore, the techniques applied in this study should be applicable to other installations for assessing relative trends in vegetation cover and land condition, even if historic ground surveys are not available. The same techniques can be applied to future imagery to continue monitoring land condition.

To quantify changes in land condition, a correlation between spectral-based indices and ground-based surveys must be established. In a recent study, correlations were established between several vegetation indices and various LCTA ground surveys (Zhuang, Shapiro, and Bagley 1993; Wu and Westervelt 1994; Senseman, Bagley, and Tweddale 1996). However, due to the lack of field data

corresponding to the imagery used in this project, it was only possible to assess relative changes in vegetation cover and land condition over time.

Mode of Technology Transfer

This technical report, data, results, and algorithms used represent the primary means of technology transfer to Fort Bliss staff.

2 Background on Satellite Data

Common commercial satellite sensors record reflectance from the Earth's surface in several regions of the electromagnetic spectrum. Depending on the intended application, different wavelengths are best suited for analyzing different aspects of the Earth-atmosphere system. For the purpose of assessing vegetation, the red and near infrared regions of the spectrum are most commonly analyzed.

Within each portion of the spectrum, different properties of vegetation control the amount of electromagnetic energy that is absorbed, transmitted, or reflected. In general, healthy vegetation has been characterized by low reflectance in the visible wavelengths (400 to 700 micrometer [μm]) and high reflectance in the near infrared wavelengths (Kauth et al. 1978; Tucker 1979; Curran 1980). Low reflectance in the visible wavelengths is due primarily to high absorption of pigments such as chlorophyll in the leaves. Low reflectance in the blue and red bands corresponds to the two chlorophyll absorption bands. However, there is a slight increase in reflectivity in the visible green portion of the spectrum (~550 μm), which explains why healthy vegetation typically appears green to the human eye.

In the near infrared region of the spectrum (700 to 1300 μm), cell structure dominates the spectral response. Unlike the visible regions, there is no strong absorption in these wavelengths and they show relatively high reflectance and scattering. Therefore, high reflectance in the near infrared wavelengths is directly proportional to plant biomass. In general, an inverse relationship exists between reflectance in the visible region, particularly in the red wavelengths, and biomass production of a plant, while reflectance in the near infrared region of the spectrum is directly proportional to plant biomass and condition (Campbell 1987).

Vegetation Indices

Several vegetation indexes have been developed to reduce multispectral scanner data observed by satellites to a single number or index, for the purpose of qualitatively and quantitatively assessing vegetation conditions (Tucker 1979; Curran 1980). Almost all vegetation indices are transformations based on the near infrared and red portions of the electromagnetic spectrum. In general, there are

two types of vegetation indices: ratio and orthogonal. Ratio indices exploit the contrasting low red reflectance and high near infrared reflectance of vegetation by simple ratios of these two bands. Orthogonal indices are based upon the "Tasseled Cap" transformation, which is a characteristic plot of red reflectance (x-axis) vs. near infrared reflectance (y-axis) that is useful for extracting relative greenness of vegetation and soil brightness (Kauth et al. 1978). Within the Tasseled Cap distribution, Kauth determined that the distribution of soil reflectance variation was confined to a "line of soils" extending from the origin at approximately 45 degrees from the x-axis (red) with soil brightness increasing with distance from the origin. Reflectance variation of vegetation is then measured perpendicularly from this line of soils in the direction of the y-axis (near infrared). This distribution was aptly named because if viewed in 3 dimensions, it resembles a cap with a tassel extending from the top. Although the original Tasseled Cap transformation was based upon Landsat Multispectral Scanner (MSS) data, the same transformations have been applied to Landsat Thematic Mapper (TM) data and other data sets. Regardless of the sensor, greenness and soil brightness indices derived from this characteristic plot are commonly referred to as Kauth-Thomas or Tasseled Cap Soil Brightness and Greenness indices.

There are numerous derivations of ratio and orthogonal vegetation indices that are beyond the scope of this report. However, all indices are similar in that they provide dimensionless values that represent relative ranges of vegetation amount or condition. In general, vegetation indices have been correlated with a number of vegetative characteristics such as biomass (Tucker 1979), percent cover (Boyd 1986; Senseman, Bagley, and Tweddale 1996), and leaf area index (Richardson and Wiegand 1977).

The Normalized Difference Vegetation Index (NDVI) is probably the most commonly applied vegetation index for assessing vegetative amount and condition (Rouse et al. 1973). In the first comprehensive study of NDVI and vegetative parameters, high coefficients of determination for a simple linear regression were found between NDVI and total wet biomass, total dry biomass, leaf water content, dry green biomass, and total chlorophyll for clipped blue grama prairie grass plots (Tucker 1979). NDVI and several other vegetation indices have also been correlated with abundance of arid shrub cover in northeast Colorado (Anderson, Hansen, and Haas 1993), Central Texas (McDaniel and Haas 1982), Central Washington (Senseman, Bagley, and Tweddale 1996) and specifically in the Chihuahuan Desert, where NDVI was correlated with abundance of mesquite, creosote, and tarbush (Duncan et al. 1993; Musick 1984, 1986).

However, a limitation of the application of NDVI in arid environments is that spectral response of the exposed soils often dominates the spectral response of

vegetation. This is due to sparse vegetation cover and high near infrared reflectance of arid soils (Graetz and Gentle 1982). Therefore, several indices have been developed to attempt to correct for this factor, including the Weighted Difference Vegetation Index (WDVI, Richardson and Wiegand 1977), the Soil-Adjusted Vegetation Index (SAVI, Huete 1988), and the Modified Soil-Adjusted Vegetation Index (MSAVI, Qi et al. 1994). These indices are designed to maximize the influence of vegetation and minimize the effect of background soil. These indices require a user-defined soil correction factor "L" as input into the indices. The constant L represents an estimate of percent vegetative cover, and therefore is often unknown. Typically, different L factors are tested and the final value is selected based on agreement with ground estimates, or an L factor is assigned based on user knowledge of the study site. In general, the L factor is difficult to objectively quantify. The Modified Soil-Adjusted Vegetation Index calculates a self-adjustable L factor calculated directly from spectral information. MSAVI also increases the sensitivity to vegetation and minimizes soil influences (Qi et al. 1994). The MSAVI accounts for possible variations of soil reflectance through an inductive method based on the opposite trends of NDVI and WDVI, thus eliminating subjective soil correction L assignments. In the original field test in cotton fields, density of the cotton canopy was predicted more accurately by MSAVI than other derivations of SAVI using remotely sensed imagery. Not only does MSAVI eliminate the requirement to estimate L, but for arid lands, MSAVI has been promoted as the best predictor of shrub cover measurements among those indices that attempt to mitigate the influence of soil reflectance (Rondeaux and Steven 1996; Senseman, Bagley, and Tweddale 1996).

Brightness Indices

Albedo (or reflectance) and soil brightness indices have also been calculated for the purpose of estimating percent vegetative cover from satellite imagery. While vegetation or greenness indices attempt to measure the reflectance of vegetation directly while minimizing soil effects, brightness indices measure the total brightness or reflectance of the Earth's surface, and therefore are more sensitive to soil background reflectance. Vegetation tends to mask the reflectance of soils, particularly in sparsely vegetated arid environments with highly reflective background soils. Therefore, an inverse relationship between brightness indices and vegetative cover has been used to estimate vegetative cover.

Albedo is defined as the ratio of all shortwave radiation reflected by the Earth's surface to solar irradiance incident on the surface. Albedo has been correlated with measurements of vegetative cover in several arid and semi-arid environments (Robinove et al. 1981; Musick 1986; Frank 1984). Planetary Albedo, or

planetary reflectance, is a measure of reflectance of the entire Earth-atmosphere system and is calculated directly from observations recorded at the satellite. Surface reflectance, or surface Albedo, is a measure of reflectance of the Earth's surface. To calculate surface Albedo or reflectance using remotely sensed observations, radiometric and atmospheric corrections must be applied to correct for atmosphere, topography, and solar geometry variations. Many times, reflectance or Albedo is calculated across all of the visible and near infrared wavelengths available. Other times, reflectance of a single spectral band, or in-band Albedo, often correlates well with vegetative cover in arid environments. In all cases, vegetative cover is measured indirectly by the relative decrease in brightness of the background soils due to vegetative cover or shadowing.

Other soil brightness indices have also been developed to assess soil brightness, and indirectly, vegetation cover. One common index is the Kauth-Thomas Soil Brightness Index (SBI, Kauth et al. 1978). The SBI is calculated based on the Tasseled Cap transformation described earlier. Similar to the Greenness Index, the SBI is derived from the characteristic plot of red vs. near infrared reflectance in spectral space. Soil brightness indices have been correlated with arid shrub cover in several studies at the Jornada Long Term Ecological Research project, which is within close proximity to Fort Bliss (Duncan et al. 1993; Musick 1984, 1986).

Change Detection

Remotely sensed imagery provides an ideal data source for assessing change in surface condition because it has high temporal frequency and large aerial coverage. Several techniques have been developed to assess change using temporal image data sets (Singh 1989). Some techniques may work better than others in different ecological settings. In arid and semi-arid environments such as Fort Bliss, the most important indicator of land condition is vegetative cover. Vegetation Indices, or Greenness Indices, and to a greater extent, Brightness Indices, have exhibited high correlation with vegetative cover in arid environments. Typically, relative increases in soil brightness or Albedo are generally associated with degradation, while relative decreases are generally associated with improvement of land condition. Conversely, relative increases in vegetation indices are associated with increased vegetative cover, and therefore improved land condition, while decreases in vegetation indices indicate a loss of vegetative cover, and therefore, high erosion potential. In many cases, a threshold is established that represents "normal" change in indices, and areas that increase or decrease beyond this threshold are identified as improved or degraded (Musick 1984,

1986; Robinove et al. 1981; Frank 1984; Price, Pyke, and Mendes 1992; and Yool, Makaio, and Watts 1997).

Simple observations of trends or differencing of indices from different image dates provides a relative measure of change in cover. Other variables may affect trends in indices, such as soil moisture, climate, and phenology of vegetation. In addition, technical errors in calibration and georegistration of temporal imagery can also bias results. However, because complete field surveys are impossible due to cost and time constraints, monitoring change in indices still provides a cost-effective method to monitor general and relative trends in land condition for military installations.

3 Study Site

A rectangular study site approximately 21 km by 9 km was chosen in the Tularosa Valley at Fort Bliss (Figure 1). U.S. Route 54 divides the study site into East and West subsections. The western edge of the study site begins near Scott Tank and extends 21 km east, crossing U.S. Route 54 and extending into the McGregor Guided Missile Range. The site was chosen to represent a contrast of historic training impact. The section west of U.S. Route 54 (hereafter called West) is in the Fort Bliss Dona Ana-Orogrande Complex and includes Maneuver Areas 5C, 5D, and parts of 4B and 4C. This area has been heavily impacted by military training and maneuvering, with very sparse vegetation remaining in the interdunal spaces between the coppice dunes. The area to the east of U.S. Route 54 (hereafter called East) is in the McGregor Guided Missile Range. This section has not been impacted by tracked and wheeled vehicle maneuvers, and therefore serves as a control for comparison with the heavily impacted maneuver areas.

The average elevation of Tularosa Valley in and around the study site is approximately 4000 ft (1220 meters [m]). The study area is comprised primarily of mesquite-covered coppice dunes. The dunes are typically oblong and average 11 m long and 6 m wide, with average interdunal spacing of 8 m. Dunes are predominantly covered by mesquite and occasional fourwing saltbush, ranging in height from 1 to 4 m with an average height of 2 m and crown density from 35 to 100 percent, averaging 55 percent. Interdunal vegetation is dominated by broom snakeweed, plains lovegrass, fluffgrass, whitestem paperflower, and isolated creosote bush (Fort Bliss Terrain Analysis [map book] 1978).

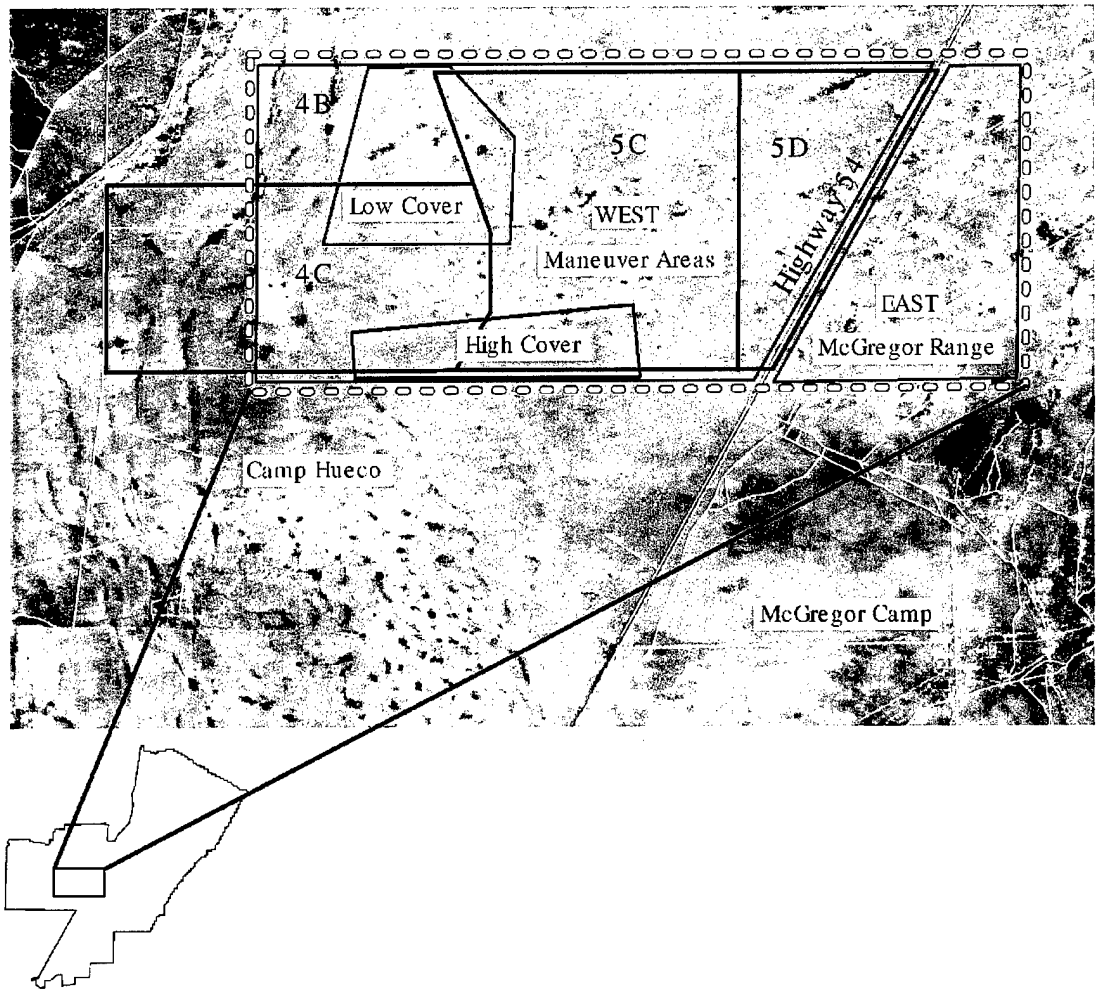

Figure 1. Location of full study site in Tularosa Basin, and East and West study areas.

4 Data Processing and Methodology

Satellite Imagery

Landsat Multi-Spectral Scanner (MSS) and Landsat Thematic Mapper (TM) imagery was compiled and analyzed for this study. The MSS sensor was launched aboard the first civil remote sensing satellite, now known as Landsat 1, in 1972. MSS collected reflectance in four (later five) spectral bands ranging from blue to near-infrared (0.5 to 1.1 μm) at an average spatial resolution of 80 m (Table 1). Two more MSS sensors were launched aboard Landsat 2 in 1975 and Landsat 3 in 1978, each with improved sensor and communication capabilities. In 1982, the TM sensor was launched along with MSS on Landsat 4. TM recorded reflected and emitted energy in seven narrower spectral bands from blue to thermal infrared (0.45 μm to 11.66 μm). A second TM sensor was launched aboard Landsat 5 in 1984. TM sensors are still in operation and images are collected daily around the world.

Table 1. Wavelength characteristics of Landsat MSS and Landsat TM sensors*.

Channel	Band width (micrometers)	Ground IFOV** (m)
Landsat 1 through 5 MSS		
1	0.5 - 0.6	80
2	0.6 - 0.7	80
3	0.7 - 0.8	80
4	0.8 - 1.1	80
Landsat 4 and 5 TM		
1	0.45 - 0.52	30
2	0.53 - 0.60	30
3	0.63 - 0.69	30
4	0.76 - 0.90	30
5	1.55 - 1.75	30
6	10.42 - 12.50	120
7	2.08 - 2.35	30

* Adopted from Table 9-2 of Lillesand and Kiefer 1987.

** Instantaneous field of view.

Sensor Differences

Although both MSS and TM sensors collect reflectance in the red and near-infrared regions of the electromagnetic spectrum, there is not a direct correspondence between the bandwidths that are collected by each sensor. MSS Band 2 is similar in spectral coverage to TM Band 3, and these two bands were used as input for red reflectance in greenness and brightness indices. MSS Band 4 is roughly similar to TM Band 4, although the MSS bandwidth is much greater. Band 4 from both sensors was used as input for near-infrared reflectance in greenness and brightness indices.

Image Compilation

Imagery was acquired from several sources and different sensors to compile an imagery data set covering a 23-year time period from 1972 through 1994. An initial review of the existing Fort Bliss imagery already available at the Engineer Research and Development Center/Construction Engineering Research Laboratory (ERDC/CERL) and the University of Wisconsin-Madison was documented. Three images of Fort Bliss were previously purchased by the UW-Madison 1994-1995 "Environmental Monitoring Practicum," which was funded by the U.S. Army Environmental Center. Temporal gaps in coverage of existing imagery were identified and an archival search of available imagery for these time periods was completed. Additional imagery was acquired to provide a single continuous temporal data set of 19 images spanning from 1972 through 1994. The late summer and early autumn (August/September/October) was identified as a target anniversary date for temporal analysis. Peak precipitation generally occurs during this time period, which in turn results in peak vegetative growth, vigor, and photosynthetic activity. However, if there was existing imagery for Fort Bliss, it was included for analysis, even if the acquisition date did not match this target anniversary date. As a result, some image acquisition dates are dispersed around this target anniversary date, and inclusion of dates that vary significantly from the target anniversary date are noted as such and are not included in analysis of temporal trends in land condition. To conduct a cross comparison of TM and MSS sensors, separate TM and MSS scenes of Fort Bliss, both acquired on 28 October 1984, were included in the study. Table 2 lists the dates and scene identification numbers of MSS and TM images used in this study.

Table 2. MSS and TM images used in this study.

MSS	
Date	**Scene ID**
6 September 1972	01196103100700001
23 December 1972	LM1035038007235890
20 October 1974	LM1035038007429390
25 November 1974	LM1035038007432990
30 September 1976	LM2035038007627490
29 September 1978	LM3035038007827290
26 December 1980	LM2035038008036190
28 June 1982	01196103100700002
5 December 1983	LM4033038008333990
28 October 1984	LM5033038008430290
TM	
28 October 1984	LT5033038008430210
15 August 1986	LT5033038008622710
19 September 1987	LT5033038008726210
24 October 1988	LT5033038008829710
29 October 1990	LT5033038009028610
4 June 1992	LT4033038009215610
18 October 1982	LT5033038009229210
19 September 1993	LT5033038009326210
9 November 1994	LT5033038009431310

Calibration

Reflectance recorded by satellites is influenced not only by the spectral properties of the Earth's surface, but also by the Earth's atmosphere, solar geometry, topographic relief, and instrument design and deterioration. To compare images collected at different times or by different sensors, these effects must be minimized. The process by which dimensionless digital numbers are converted to physical units of reflectance is called radiometric correction or calibration. Several radiometric calibration techniques of varying complexity can be applied. In many cases, complete radiometric calibration requires field measurements of atmospheric influences at the time of image acquisition. In addition, information on solar zenith angle, topography of the Earth's surface, and radiometric qualities of the sensor are needed. Solar zenith angle and radiometric information are recorded in the image header files. Prelaunch radiometric sensitivity of the sensor is also published information. For this study, in-situ measurements of atmospheric scattering were unavailable. Therefore, an alternative method was used to estimate and correct for atmospheric scattering in the temporal data set.

A large pond in Sunlake Park near El Paso, Texas, was selected to represent a relatively stable target over the entire period from 1972 through 1994. For each image, the mean value for all the pixels within the area defined by Sunlake Park pond were calculated for each band (see Appendix A). In the MSS images, the means were relatively stable for all bands for all years. For the TM images, the means were relatively stable in bands 1 through 4 but varied greatly for bands 5 and 6.

Any differences in observed reflectance values for the pond from different dates were assumed to be due to a change in atmospheric attenuation. Using these mean values for the pond for each band, the minimum mean for each band was identified and used as a standard or baseline. This minimum mean was subtracted from the mean values observed in the same band for the other dates. The resulting differences, or offsets, were assumed to be the atmospheric influence present in each image. These offsets for each band were then subtracted from all pixel values in the respective images, resulting in an atmospherically corrected temporal data set (Scarpace et al. 1995). It is recognized that a natural water body is not an ideal stable target for the purpose of image calibration, as there may have been variations in reflectance of the pond due to depth and turbidity of the water. However, there were limited stable surfaces that could be identified in each scene of the temporal data set. Therefore, the pond was chosen for calibration purposes, and any variations in pond reflectance due to actual changes in the lake itself were assumed to be minimal.

Solar illumination differences due to aspect from varying topography were assumed to be minimal for the study site, and therefore were not considered in the analysis. Solar zenith angles were acquired from image header files. When available, radiometric offset and gain values were also acquired from image headers. If unavailable, published, pre-launch radiometric offset and gain values were used to calculate reflectance.

Noise Reduction

Systematic horizontal strips of bad data were evident in several of the images. These problems were particularly evident in the MSS imagery, although some noise is also apparent in the TM imagery. Striping of MSS imagery is a result of a known problem with improper synchronization of scan lines by the sensor. A periodic noise removal algorithm (available in Earth Resources Data Analysis Systems, Inc. [ERDAS]) Imagine software) was applied to striped images in an attempt to remove or minimize noise. The periodic noise removal performs an enhancement of the image based on a Fourier transform. The original striped

image is first divided into 128 by 128 pixel blocks. The Fourier transform for each block is calculated and the log-magnitudes of each Fast Fourier Transform (FFT) block are averaged. The averaging removes or significantly reduces all of the periodic interference (ERDAS 1993). However, the periodic noise removal changed the actual digital numbers in the imagery, and therefore had a minor effect on vegetation and soil brightness indices.

Georeferencing

Once imagery was compiled and corrected for atmospheric and problem scan lines, the images were georeferenced to a Universal Transverse Mercator (UTM) coordinate system. Satellite imagery is acquired in raw form, and therefore is not referenced to an established coordinate system. Georectification is required to locate reflectance values of individual pixels to a known coordinate system. Once an image is georeferenced, reflectance values can be related to a geographic location on the ground. Typically, georeferenced imagery is entered as a data layer in a geographic information system (GIS) for subsequent spatial analysis with other geographic information, including additional imagery. To georeference an image, precise geographic coordinates of identifiable ground control points (GCPs) must be located in the imagery. Geographic coordinates for control points can be obtained by locating the same points in another map that is already georeferenced to a coordinate system, or the coordinates can be collected in the field using Global Positioning System (GPS) technology. Based on known control points, a transformation matrix is calculated and used to resample each pixel or data element to a known coordinate system.

The University of Wisconsin-Madison 1994-1995 "Environmental Monitoring Practicum" collected coordinates for ground control points using GPS technology and georeferenced the 4 June 1992 image to (1) a UTM coordinate system and projection, (2) Zone 13, and (3) Northern Hemisphere Clarke 1866 Spheroid. All other images were georeferenced to this base image. Although some images of Fort Bliss had been georeferenced prior to this study, the registration was of questionable quality. Therefore, original source imagery was located, control points were identified, and the images were georeferenced to the base 1992 TM image.

Stable GCPs such as road intersections and buildings were located in the raw source image and the base 1992 image. Once a suitable number of GCPs were selected, a transformation matrix and corresponding measure of fit, called the Root Mean Square (RMS) error, was calculated. A transformation matrix is a set of coefficients used to convert pixels to georeferenced coordinates. RMS error is

the distance between the desired output coordinate for a GCP and the actual output coordinate for the same point if that point were to be transformed with the current transformation matrix. Therefore, when selecting and evaluating GCPs, the goal was to minimize RMS error while distributing GCPs evenly across the image. RMS error can be measured in meters on the ground or in a fraction of the smallest picture element (pixel) in the image. Using TM imagery with 30-m spatial resolution as an example, an RMS error of .333 would indicate that the base and source images are spatially misregistered by one-third of a pixel (or 10 meters). A maximum acceptable RMS error of .30 was established for all georectifications in this study.

An attempt was made to use the same GCPs in successive images when possible. However, over the time period of this study, many landmarks that were clearly identifiable in the 1992 base image could not be located in imagery from the early 1970s. Therefore, new GCPs had to be located; the same control points were not used for all images in the temporal data set.

Once an acceptable set of GCPs was located in the imagery, a first order polynomial transformation was applied and the raw image pixels were resampled to match the 1992 image using a nearest neighbor resampling in ERDAS Imagine.

Final evaluation involved visual comparison of the newly georeferenced image with the 1992 base image. In the event that georegistration appeared inaccurate, GCPs with unusually high RMS errors were eliminated and different control points were selected. This process was repeated until low RMS errors were reported and visual inspection confirmed an accurate georectification.

Study Site Subset

Once all images in the temporal data set were georeferenced to a common coordinate system, an area corresponding to the study site was extracted from each image. For MSS imagery, the resulting image subsets matching the study area were 259 by 109 pixels, while subsets from the TM imagery were 691 by 291 pixels.

Index Calculations

Four vegetation or greenness indices and four brightness indices were calculated for each of 19 images in the temporal data set, which spanned from 1972 through 1994. Each index was selected based on its sensitivity to percent vegetative

cover as summarized in previous literature (Tucker 1979; Robinove et al. 1981; McDaniel and Haas, 1982; Musick 1984; Huete 1988; Duncan et al. 1993; Qi et al. 1994). The vegetation or greenness indices calculated were the Normalized Difference Vegetation Index (NDVI), the "Tasseled Cap" Greenness Index, and two derivations of the Soil-Adjusted Vegetation Index: SAVI and a Modified SAVI (MSAVI2). The brightness indices calculated were Albedo (or reflectance) over all visible and near-infrared bands, in-band Albedo in the red and near-infrared wavelengths individually, and the "Tasseled Cap" Soil Brightness Index. All processing was done under the image processing software package Imagine, which is distributed by ERDAS. A graphical model in Imagine was used to calculate the indices as follows:

1. NDVI (Rouse et al. 1974)

$$NDVI = \frac{NIR - red}{NIR + red}$$

2. SAVI (Huete 1988)

$$SAVI = \frac{NIR - red}{NIR + red + L}(1 + L)$$

3. MSAVI2 (Qi et al. 1994)

$$MSAVI2 = \frac{1}{2}\left(2(NIR + 1) - \sqrt{(2 \times NIR + 1)^2 - 8(NIR - red)}\right)$$

4. Tasseled Cap Greenness (TCG) Vegetation Index

For MSS:

TCG = (-0.283)(MSS1) - (0.660)(MSS2) + (0.577)(MSS3) + (0.388)(MSS4)

For TM4:

TCG = (-0.285)(TM1) - (.244)(TM2) - (.544)(TM3) + (.724)(TM4) + (.084)(TM5) - (0.180)(TM7)

For TM5:

TCG = (-0.273)(TM1) - (.217)(TM2) - (.551)(TM3) + (.722)(TM4) + (.073)(TM5) - (0.165)(TM7)

5. Albedo

Prior to calculation of Albedo (or reflectance), digital numbers were converted to spectral band radiance for MSS and TM imagery using (Markham and Barker 1986):

$$L_\lambda = \frac{L\min_\lambda + [L\max_\lambda - L\min_\lambda]DN}{D\max} \qquad \text{Equation 1}$$

where: Lmin = spectral radiance of each band at DN = 0 in

$mWcm^{-2}Sr^{-1}:m^{-1}$

Lmax = spectral radiance of each band at DN=255 (DN= 127 for MSS) in

$mWcm^{-2}Sr^{-1}:m^{-1}$

Dmax = range of rescaled radiance in DN

DN = input digital number.

Once spectral radiance was calculated according to Equation 1, Albedo was calculated as the ratio of reflected solar radiation to incoming solar irradiance:

$$\rho = \frac{\pi L_\lambda d^2}{E_\lambda \cos 6} \qquad \text{Equation 2}$$

where: L_8 = spectral radiance in $mWcm^{-2}Sr^{-1}:m^{-1}$ (from Equation 1)

d = Earth - sun distance in astronomical units

E_8 = exoatmospheric spectral irradiance at the top of the atmosphere in $mWcm^{-2}:m^{-1}$

2 = solar zenith angle.

Radiance is derived from digital numbers recorded on computer-compatible tapes. Exoatmospheric spectral irradiances at the top of the atmosphere are estimates derived from Markham and Barker (1986). Correcting exoatmospheric solar irradiance in the denominator by cos 2 normalizes scenes to an overhead or nadir sun angle and accounts for differences in solar irradiance for the time of day and day of the year (Robinove et al. 1981).

Total reflectance or planetary Albedo was calculated by integrating spectral radiance and irradiances across all of the visible and the near- and middle-infrared bands. Planetary Albedo for MSS was integrated across all 4 bands, while planetary Albedo for TM imagery was integrated across only bands 1 through 5. In-band planetary Albedo for red and near-infrared bands was calculated in the same manner as total reflectance or planetary Albedo (Equation 1). However, red and near-infrared reflectances were calculated using radiance and irradiances in only the red and near-infrared wavelengths.

6. Tasseled Cap Brightness (TCB) Index

For MSS:

$$TCB = (.332)(MSS4) + (.603)(MSS5) + (.675)(MSS6) + (.262)(MSS7)$$

For TM4:

$$TCB = (.304)(TM1) + (.279)(TM2) + (.474)(TM3) + (.559)(TM4) + (.508)(TM5) + (.186)\ (TM7)$$

For TM5:

$$TCB = (.291)(TM1) + (.249)(TM2) + (.481)(TM3) + (.557)(TM4) + (.444)(TM5) + (.171)\ (TM7)$$

5 Analysis and Results

A temporal data set of 19 satellite images spanning 23 years was compiled and analyzed to assess historical trends in relative land condition and contrasting land uses over this time period for a specific study site at Fort Bliss, Texas. However, a secondary product of this research is a complete temporal data set for the entire installation over this same time period. Spanning from 1972 through 1994, the data set includes imagery ranging from the earliest commercially available satellite platform (Landsat 1 MSS) to a satellite platform (Landsat 5 TM) that is still functional today. For most years in this temporal data set, complete coverage of the entire installation does exist. Many images were compiled from archival information at ERDC/CERL, while others were purchased as part of this project. Because of the size and location of Fort Bliss, several images are required to provide complete geographic coverage of the installation. For example, three Landsat TM scenes are required for complete coverage because of the orbit of the Landsat satellite and swath size of the TM sensor. However, two TM scenes provide close to 95 percent coverage of the installation. A third image is required to cover the extreme northeast corner of Fort Bliss, and in many cases, was not available from archival imagery of the installation. For the years in which imagery was acquired specifically for this project, a single TM scene was selected, which provided coverage of the study site. Therefore, for those years, complete coverage of the entire installation is not available.

The results summarized in this chapter are specifically focused on a retrospective analysis of a specific study site, as described in Chapter 3, and were not compiled for the entire installation. The analysis is focused on historical trends and spatial patterns of remotely sensed indices, which are indicators of vegetative cover, and indirectly, land condition for the entire study site, and also focused on areas of contrasting land use within the study site.

Historical Trends

Eight remotely sensed indices were calculated from each image date for the study site. Four of the indices were vegetation indices or greenness indices: (1) the Normalized Difference Vegetation Index (NDVI), (2) the "Tasseled Cap" Greenness Index (TCG), (3) the Soil-Adjusted Vegetation Index (SAVI), and (4) the Modified SAVI (MSAVI2). The four remaining indices were brightness

indices: (1) Albedo, (2) the "Tasseled Cap" Brightness Index (TCB), (3) Red Reflectance, and (4) Near-Infrared Reflectance.

When analyzing a single image, radiometric and atmospheric calibration was not necessary. However, because the primary goal was to analyze a temporal sequence of images collected from different platforms and under presumably different atmospheric conditions, radiometric and atmospheric corrections were applied to the original Digital Numbers (DNs), and all indices were calculated using calibrated reflectance data. The resulting indices calculated from calibrated reflectance values were dimensionless numbers. Therefore, the indices were ideal for comparisons between pixels in a single image, or in this case, when calibrated, for comparison between pixels representing the same geographic area in a temporal sequence. Similarly, reflectance in the red and near-infrared wavelengths was also calibrated for comparison over the same temporal sequence. However, radiometric and atmospheric calibration is not an exact science, and although procedures were followed to calibrate image data from different dates for the purpose of isolating actual differences of the Earth's surface, the results should be used only for identifying general and relative trends in surface conditions.

Especially problematic to this research was the fact that imagery was compiled from Landsat MSS and TM sensors, which have significantly different spatial and spectral characteristics. Due to differences between these sensors, comparison of index values spanning between MSS and TM dates may not provide an accurate representation of actual surface conditions over this entire time period. Because different spatial and spectral resolution imagery captures a different mixture of landcover components within a single pixel (or data element), the resulting indices calculated from MSS data are not suitable for comparison with indices calculated from TM data. Therefore, the temporal sequence of MSS imagery spanning from 1972 through 1984 was analyzed and is presented separately from the temporal sequence of TM imagery, which spans from 1984 through 1994.

Appendix B lists the mean, standard deviation, minimum and maximum index values, and reflectance values for the entire study site for each image date and for each of the eight greenness and brightness indices. Appendix B also includes similar statistics for subsets of the study area, which are discussed later in this report. Although eight indices were tabulated for each date, a final group of four indices (Albedo, Tasseled Cap Brightness, Red Reflectance, and MSAVI2) were selected for more detailed analysis. These indices were selected based on related research and literature (Musick 1984; Robinove et al. 1981; Duncan et al. 1993; Pickup, Chewings, and Nelson 1993), which indicated that they would be most

sensitive to vegetative cover and land condition, and therefore, would be optimal for analyzing trends in land condition over time. Mean index values for the entire study site for each of these four indices were plotted for each image date in Figures 2 and 3.

Initial examination of the three mean brightness indices (Albedo, Red Reflectance, and "Tasseled Cap") from 1984 through 1994 using TM imagery (Figure 3) reveals a similar pattern. Each index dropped sharply in both 1986 and 1992. However, note that the 1992 image was collected in June, which varies considerably from the remaining acquisition dates that span from August through October. Ideally, when evaluating a temporal sequence of imagery to detect change, images should be acquired as close as possible to the same anniversary date to minimize phenological differences between scenes. Therefore, when evaluating trends over this time period, the June 1992 data should be interpreted with caution. The 1986 scene was collected in August, which represents the earliest part of the targeted image acquisition time period. Therefore, phenological differences may also explain the relatively low brightness indices for this date (Albedo = 11.91, TCB = 44.64, Red = 11.89), yet the indices are still considerably lower than the 1988 scene (Albedo = 14.22, TCB = 52.52, Red = 14.45), which was also acquired in August.

Another critical consideration when evaluating trends in spectral indices to assess land condition is climatic information, such as antecedent precipitation leading up to the image acquisition date. Precipitation affects spectral brightness indices in two ways. First, any precipitation that occurs close to the acquisition date of the image may result in increased soil moisture that may act to decrease brightness, as wet or damp soils are darker than dry soils. Second, increased precipitation usually results in an increase in the amount and vigor of perennials and annuals, which may also result in decreased brightness (Robinove et al. 1981). Robinove and associates revealed that the major determining factor in a change in brightness measures such as Albedo, for example, was antecedent precipitation for 7 or more months leading up to the later date in the temporal sequence over which change in Albedo is observed. These results have not been validated with rigorous statistical analysis, but they do demonstrate the importance of considering climatic variables when analyzing change in spectral indices. Therefore, monthly precipitation data was collected from 1972 through 1995 from El Paso Airport, which is a few kilometers south of the study area (Figure 4). Although the majority of precipitation at Fort Bliss falls from late summer and early autumn thunderstorms, which are often isolated, the El Paso precipitation data does provide a general estimate of precipitation at the study site.

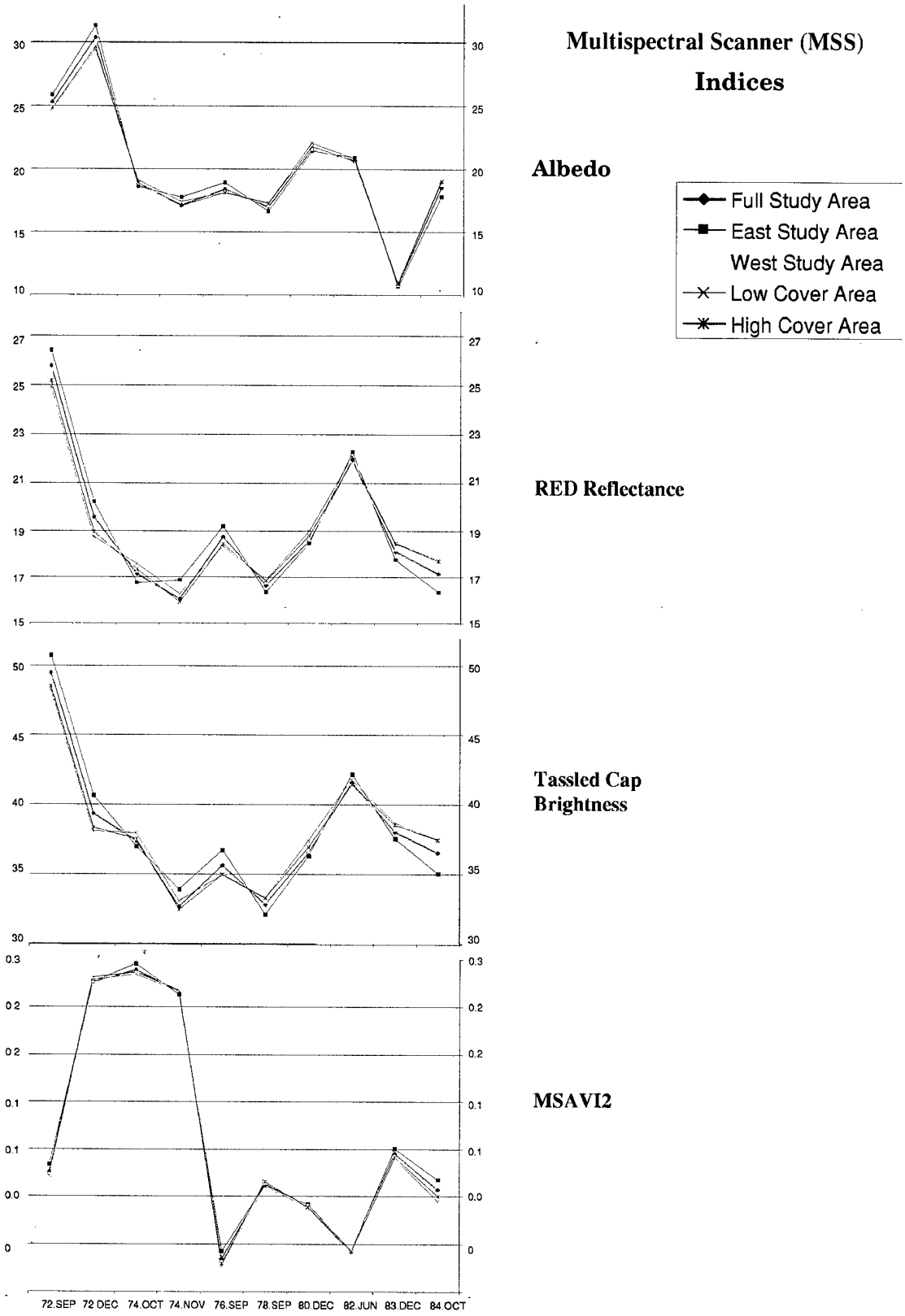

Figure 2. Trends in spectral indices from MSS imagery (1972 through 1984).

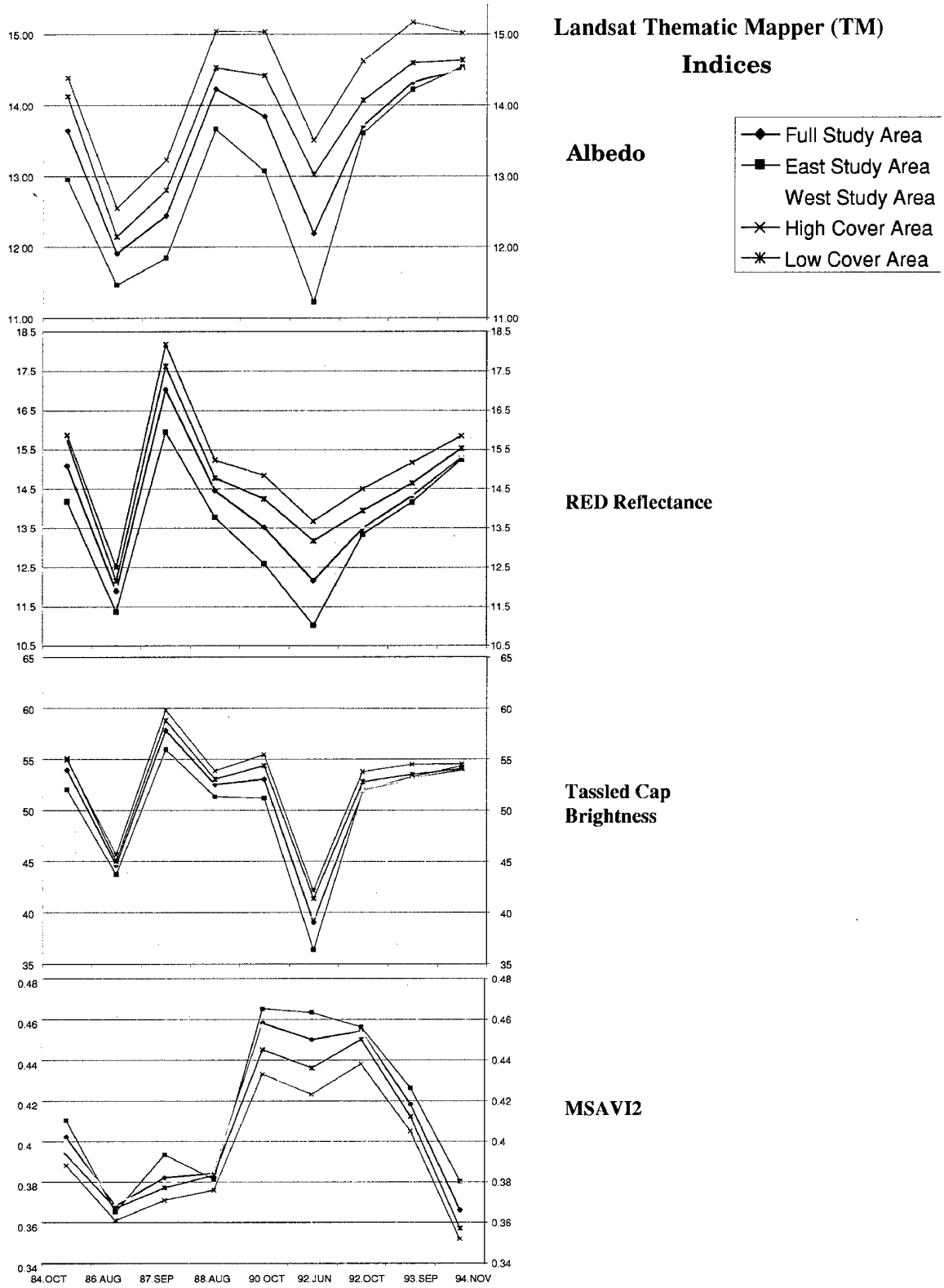

Figure 3. Trends in spectral indices from TM imagery (1984 through 1994).

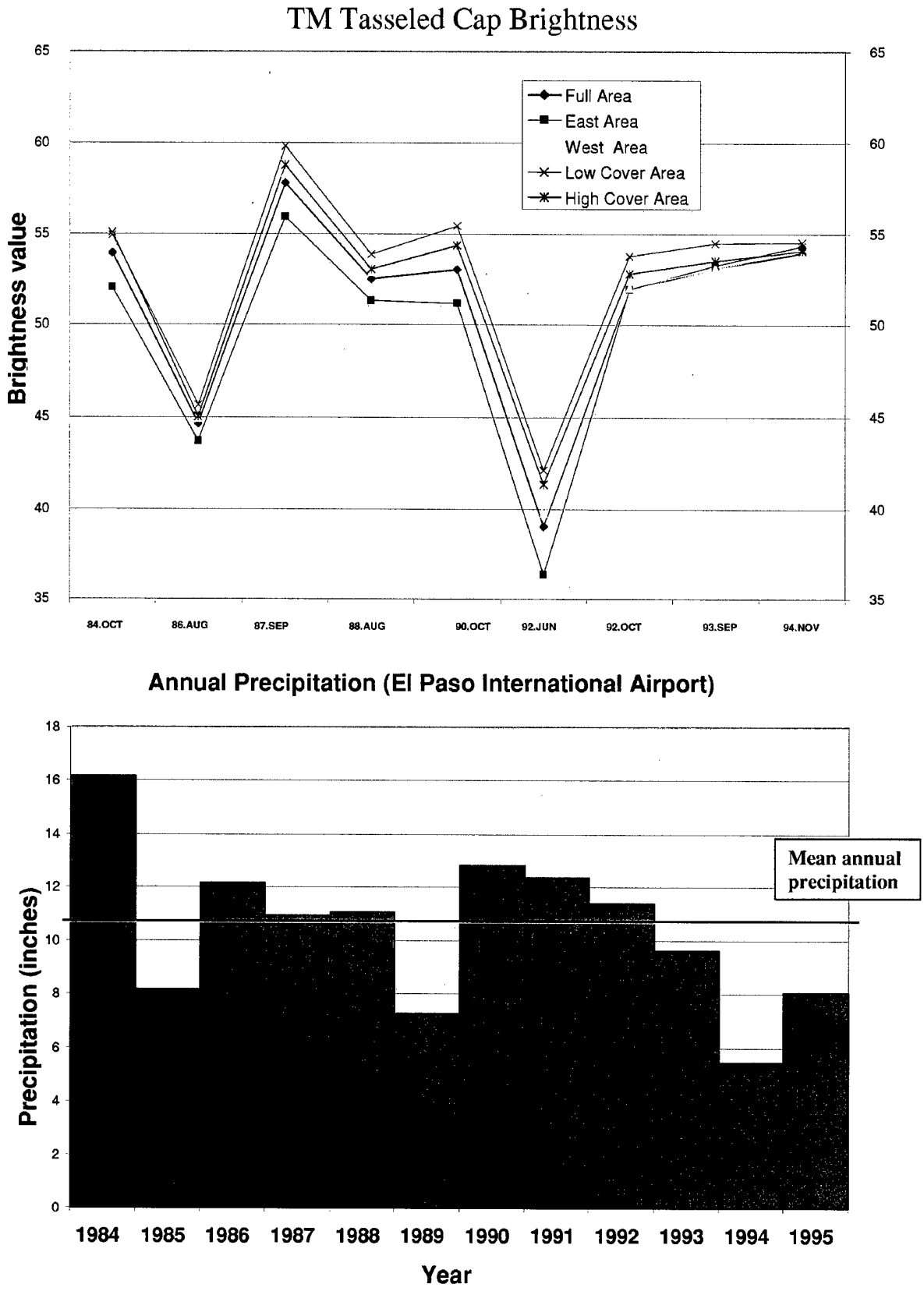

Figure 4. Landsat TM Tasseled Cap brightness and annual precipitation (1984 through 1995).

Although the June 1992 scene was not considered in evaluating the overall trend of indices (because June varies from the remaining acquisition dates), precipitation records indicate a relatively high amount of precipitation was recorded in May 1992 (4.22 in. [10.72 cm]), which may partially explain the significantly lower brightness indices observed for this date. Similarly, a relatively high amount of precipitation was recorded in June (3.05 in. [7.75 cm]) and July (2.66 in. [6.76 cm]) of 1986, again possibly explaining the observed decrease in brightness in the August 1986 image.

Conversely, a significant increase in brightness was observed for TCB and Red Reflectance in 1987 (Figure 3). Although precipitation for September 1987 (image acquisition date) was below the mean precipitation recorded in September for the time period of this study (0.89 in. [2.26 cm]), and precipitation in July was also below average (0.64 in. [1.63 cm]), total antecedent precipitation leading up to the acquisition date appeared to be normal or even slightly above normal. Therefore, it does not appear that this increase in brightness can be totally explained by existing precipitation records; more detailed climatic data would be required to confirm this observation. It is possible that the increase in detected brightness in 1987 may be the result of increased training impact between 1986 and 1987, relative to other temporal sequences observed. However, cause and effect requires more detailed field data, including climatic data, soil moisture, and information on the intensity and geographic extent of training exercises during this time period. Note that although spectral brightness peaked in 1987 according to Red Reflectance and TCB, the same increase was not evident in Albedo, which indicated a larger increase between 1987 and 1988 (Figure 3).

In contrast to these brightness indices, a single greenness index (MSAVI2) was also evaluated. As described earlier, brightness indices are usually more indicative of land condition than greenness indices in arid environments with relatively sparse vegetation cover. Spectral greenness and brightness indices are usually inversely proportional to each other in arid environments. An increase in brightness and decrease in greenness is usually associated with degradation, while a decrease in brightness and increase in greenness is usually associated with an increase in vegetative cover and improvement in land condition. However, in arid environments where vegetative cover does not exceed 30 to 35 percent background soil brightness dominates the spectral response, and therefore greenness indices typically do not correlate well with abundance of vegetative cover. Despite these recognized limitations, MSAVI2 was evaluated for comparison.

Based on the typical inverse relationship between brightness and greenness indices, one would expect increases in MSAVI2 for time periods where a decrease

in brightness was observed, and vice versa. However, this only occurred between 1992 to 1993, and 1993 to 1994, when MSAVI decreased and all three brightness indices increased, and also in 1987 to 1988, and 1988 to 1990, where MSAVI increased, and some, but not all, of the brightness indices decreased (Figure 3). In June 1992, when brightness values were relatively low, MSAVI2 values were relatively high. However, in August 1986, when brightness values were relatively low, MSAVI2 values were also relatively low.

The minimum MSAVI2 value was recorded in 1994. Acquired at the onset of senescence, this image, as well as the November 1992 image, should be interpreted with caution, or perhaps eliminated from consideration when evaluating trends.

Based on previous literature (Robinove et al. 1981; Musick 1984; Duncan et al. 1993), and the unexpected trends in MSAVI2 when compared with trends in brightness indices, it was determined that MSAVI2, as well as other greenness indices that were evaluated over the same time period, were not good indicators of vegetative cover and land condition. However, the relationship between MSAVI2 and the brightness indices is discussed further when land use patterns are considered.

Examination of all three mean brightness indices from 1972 to 1984 using MSS imagery reveals a similar pattern, especially between Red Reflectance and TCB (Figure 2). Both Red Reflectance and TCB indices indicated that September 1972 had the highest reflectance or brightness over this time period, followed by a significant decrease in brightness in December 1972. Albedo was also very high in September 1972, and increased even higher by December 1972, even though Red and TCB indicated a large decrease in brightness over this 3-month time period. Similar to Red and TCB, Albedo decreased significantly between September 1972 and October 1974. Although there was some continued slight variation in the trend of brightness indices from 1974 to 1984, the September 1972 image and, to a lesser extent, the June 1982 image were the only two dates that exhibited relatively high brightness indices. As mentioned earlier, the June image should be interpreted with caution, as it varies considerably from the target acquisition dates (August through October). Phenological differences between the relatively dry period of mid-summer (June) and the wet season (August to October) scenes are the most likely explanation for the relatively high brightness indices observed for June 1982.

Precipitation records may provide some explanation for the rapid decrease in brightness indices between September 1972 and November 1974. 1974 was the second wettest on record of the 23 years observed by this study (13.95 in. [35.43 cm]). Also, September 1974, which was 1 month prior to the image acquisition

date, was the wettest month on record over this same time period, with 6.68 inches [16.97 cm] of rainfall. This amount of precipitation undoubtedly resulted in a significant increase in vegetative cover, growth, and vigor in the following month, as well as an increase in soil moisture, both of which would explain the observed decrease in brightness during this time period. The relatively high amount of precipitation recorded in September 1978 may also explain the relative decrease in observed brightness or reflectance in the September 1978 image.

In contrast to these brightness indices, the greenness index (MSAVI2) increased significantly between September 1972 and October 1974. Again, this would support the hypothesis that this trend is most likely attributable to a significant increase in precipitation and moisture availability that resulted in a substantial increase in vegetative cover, growth, and vigor over this time period.

Unlike comparisons between trends in brightness and greenness indices derived from TM imagery, the typical inverse relationship between brightness and greenness indices was evident for most of the time periods observed with MSS imagery. In addition to the expected inverse trends in brightness (decrease) and greenness (increase) between 1972 and 1974, the trends reversed and were still inverse to each other between September 1978 and June 1982, when brightness indices increased and greenness indices decreases.

Land Use Comparison

In addition to assessing relative, temporal trends in land condition using remotely sensed spectral indices for the entire study area, a second goal of this research was to compare trends for land areas with contrasting historical land uses. As described in Chapter 3, U.S. Highway 54 served as a dividing line between two areas of distinctively different historical land use in the study area. The subset of the entire study area that is west of U.S. Route 54 (hereafter called West) is in the Fort Bliss Dona Ana-Orogrande Complex. This subset includes most of Maneuver Areas 5C, 5D, and parts of 4B and 4C, all of which have been heavily impacted by tracked and wheeled military training and maneuvering from 1972 through 1994. The subset area to the east of U.S. Route 54 (hereafter called East) is in the McGregor Guided Missile Range. This section has not been impacted by tracked and wheeled military training and maneuvers, and therefore served as a control for comparison with the heavily impacted maneuver areas.

Appendix B summarizes the same statistics for each of the four indices for the East and West subsets that were summarized for the entire study area. In addi-

tion, mean index values for East and West for the indices evaluated for the entire study area were also plotted for each image date in Figures 2 and 3.

Initial examination of all three mean brightness indices derived from TM imagery for the East and West areas from 1984 through 1994 revealed a trend similar to that observed for the full study area. Extremes in mean values for the East and West land areas occurred during the same years as those observed for the full study area. Trends in mean brightness values for the east and west areas were very similar to the trends observed for the full study area. This suggests that for the years in which extremes were observed, they were the result of climatic or phenological differences that occurred uniformly across the entire study area, and were not a result of military impacts. If an increase in brightness for the entire study area for certain years was an indicator of increased training impact, there should have been an observable difference in response between the impacted (West) and nonimpacted (East). This difference was not observed. One observation of potential significance was that the difference in mean brightness between East and West decreased substantially beginning in 1992 and continuing through 1994. This may indicate two possible trends: either vegetative cover was increasing in the West relative to the East, or was decreasing in the East relative to the West. Since the overall trend in brightness indices increased between 1992 and 1994, this would indicate that the latter is more likely, with vegetative cover decreasing in both areas, but decreasing more rapidly in the East. Records indicated that annual precipitation was below the mean annual precipitation for both 1993 and 1994, with 1994 being the driest year (5.48 in. [13.92]) of all years observed in this study. This may explain the overall trend of increased brightness for the entire study area, but would not explain the greater increase in brightness for the East.

Not only was the difference in brightness between East and West relatively consistent for all years, with the exception of 1992 through 1994, but the West area had a higher brightness index than the East area for each year observed. Conversely, the East area had a higher greenness index than the West area for each year observed. This observed difference between East and West corresponds well with what was expected based on the historical land use of each area. The West has been more heavily impacted by tracked and wheeled vehicles than the East, and therefore, it was expected that there would be relatively less vegetative cover and more exposed and disturbed soil in the West than in the East. Consequently, the West area should have a higher brightness index and lower greenness index than the East area.

One final comparison of land areas within the full study area was observed for two areas that did not have a clearly different historical land use, but instead

were visually identified on the index images as contrasting areas. Within the West area were two visibly distinct subareas; the first appeared more heavily impacted and is referred to as Low Cover in this study, the second area, High Cover, was identified as less impacted.

Similar to comparisons made between East and West, the same statistics for these two subareas are summarized in Appendix B and the annual mean index values for these areas are plotted in Figures 2 and 3. Visually observed differences between these two areas were confirmed by assessing differences between brightness values for each area for each year observed. The Low Cover area exhibited the highest brightness index of all areas observed in this study, including the full study area, the East and West study areas, and the visually identified High Cover area within the West study area. Similarly, the Low Cover area also had the lowest greenness index (MSAVI2) of all areas observed in this study. Examination of all three mean brightness indices for the Low Cover and High Cover areas from 1984 through 1994 using TM imagery (Figure 3) revealed a trend similar to that of the full study area and the East and West areas. Extremes in mean values for the East and West land areas occurred during the same years as those observed for the full study area. Similar to earlier conclusions, this would suggest that observed extremes were probably the result of climatic or phenological differences that occurred uniformly across the entire study area rather than to the varying degree of military impacts that may have occurred in the Low Cover and High Cover areas.

Spatial Patterns

One final objective of this research was to identify any spatial patterns of small scale, gross level change that were evident in the temporal, archival multispectral image data set. Several commonly used change detection methods have been applied to temporal image data sets with varying results, as described in Chapter 2. The most commonly applied method, and the one used in this research, is referred to as image differencing.

As the name suggests, images from two different dates are spatially coregistered to each other and subtracted using image algebra. The difference between pixel values between the two dates in a temporal sequence is then assigned as the pixel value in the difference image. If the intent is to monitor some specific aspect of the Earth's surface, such as vegetative cover and/or exposed soil, it is advantageous to first calculate an index from the two original image dates that provides a good indicator of the variable of interest on the surface. In this case, the index images are subtracted, rather than the digital numbers (DNs) in the

original images. At a minimum, the DNs should always be calibrated to account for possible atmospheric and radiometric differences between image acquisition dates. In many cases, a threshold is established that represents "normal" change in indices between two dates. Areas that increase or decrease beyond this threshold are identified as improved or degraded. Establishing a threshold allows identification of areas that have increased or decreased beyond the mean change between two image dates. This serves to eliminate changes that occurred uniformly across an image, such as climatic or phenological change, and isolates areas where there has been an actual change in land condition. Selection of similar image acquisition dates for different years helps to eliminate or minimize phenological differences as well.

Using image index differencing, patterns of change were identified for three different temporal sequences using TM imagery. Brightness indices, and not Greenness indices, were selected for image differencing based on previous research and literature (Robinove et al. 1981; Musick 1984; Duncan et al. 1993), which indicates that brightness indices are best for monitoring vegetative cover in arid environments. Differences between several brightness indices were mapped and evaluated, and it was determined that similar patterns were detected using different brightness indices. Red Reflectance and TCB, were selected for detailed analysis and presentation. Changes in these two indices were mapped between 1987 to 1990, 1990 to 1993, and overall from 1987 to 1993. For each time sequence, the mean difference between the two image dates was determined, and areas that increased or decreased beyond 2 standard deviations from the mean change were mapped within the study area. These images are presented in Figures 5, 6, and 7.

As mentioned earlier, an increase in a brightness index is usually associated with degradation or loss of vegetative cover, while a decrease in a brightness index is usually associated with an increase in vegetative cover. Therefore, those areas that decreased by more than 2 standard deviations from the mean decrease between the two dates, or those areas that may have increased, but by less than 2 standard deviations from the mean increase were highlighted in green on the map to signify a potential increase in vegetative cover and improvement in land condition. Conversely, those areas that increased more than 2 standard deviations from the mean increase, or those areas that may have decreased, but by less than 2 standard deviations from the mean decrease were highlighted in red on the map to signify a potential decrease in vegetative cover and degradation. However, these areas of delineated change must be interpreted with caution, as there was no field data to verify and validate the observed changes. Therefore, cause and effect was difficult, if not impossible, to establish. Several other factors that are not related to actual change in land condition may

to these areas of observed change. Simple spatial registration or atmospheric calibration errors between image dates could result in the misclassification of change. Spatial registration errors are most noticeable along linear features such as roads or other features with a high contrast edge between two land cover types. In addition, even though images of similar anniversary dates were analyzed, there may still have been phenological differences between the dates. And, there may still have been differences in climatic conditions between the two seasons, including differences in precipitation in the preceding months, or even a very recent precipitation event, which would have resulted in increased soil moisture for one of the dates.

Between 1987 and 1990, there was a decrease in mean brightness for both TCB (-4.83) and Red Reflectance (-23.41) for the entire study area. Figure 5 shows a map of those areas of extreme change (+/- 2 s.d. from the mean change) for TCB and Red Reflectance. Green highlighting identifies those areas that became much less bright or less reflective over this time period; conversely, red highlighting identifies those areas that became much brighter or more reflective over this same time period. Patterns of extreme change were very similar for both brightness indices, which was expected. Several areas of observed extreme change were visited in the field. Although field verification was conducted several years after the time of the observed change, field observations confirmed that, in most cases, areas of extreme change seemed to occur in depressions, or isolated areas of high productivity and vegetative cover, or in areas of extremely low vegetative cover or completely exposed soils.

Between 1987 and 1990, those areas that decreased much less than the mean decrease in brightness for the study area (highlighted in green) appeared to occur in isolated areas of extremely low vegetative cover, or bare ground. This would generally indicate an increase in vegetative cover or decrease in exposed soils for these areas. Precipitation records indicate that precipitation before the 1990 date was significantly higher than precipitation before the 1987 date. Therefore, these areas would have had more moisture available, and as a result, one would expect an increase in vegetative cover, growth, and vigor in these areas in 1990 relative to 1987. It is likely that these areas experienced a combination of green-up of perennials and annuals, an increase in soil moisture, and possibly an increase in shadows, which may have caused these areas to appear significantly darker in 1990. Areas where these extreme changes were most evident were on the McGregor Range and directly west of Highway 54 in Maneuver Area 5D, as well as a few isolated areas of extremely low cover in Maneuver Area 5C. These areas also occurred along many of the roads and trails. There may have been an increase in soil moisture in these areas, or the extreme change may

also have been the result of a slight spatial registration error between the two image dates.

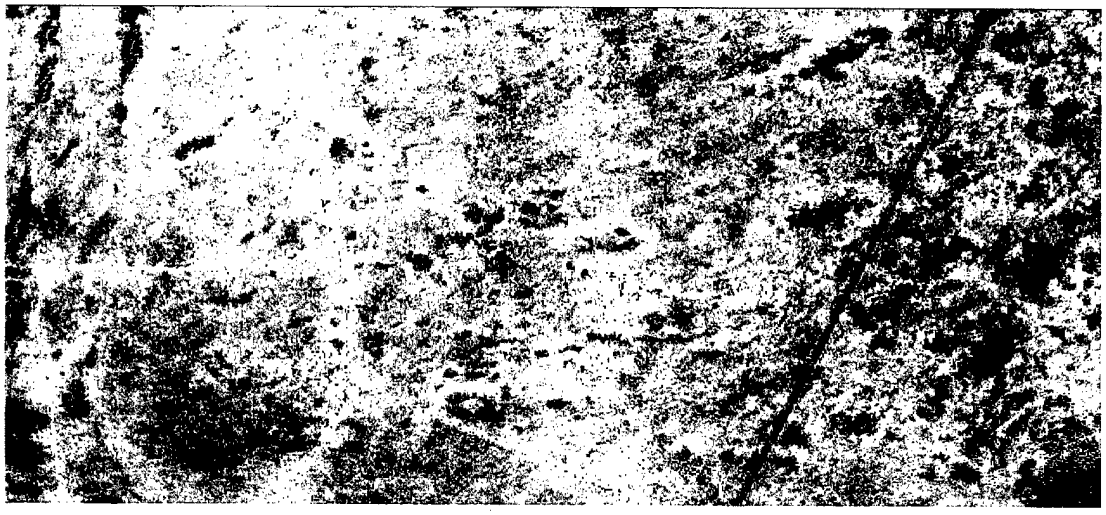

Legend:

- Decrease in Tasseled-Cap Brightness Index greater than 2 standard deviations from mean change between 1987 and 1990.
- Increase in Tassled-Cap Brightness Index greater than 2 standard deviations from mean change between 1987 and 1990.

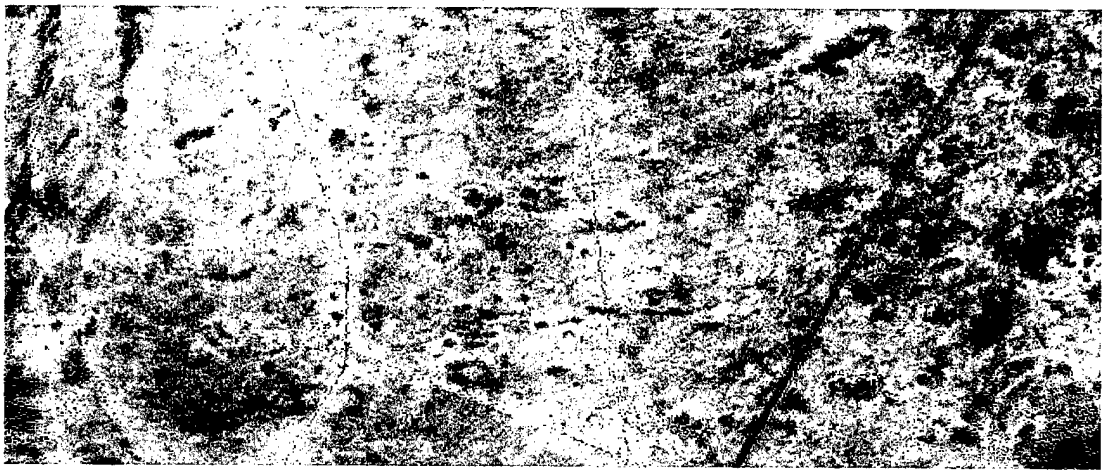

Legend:

- Decrease in Landsat TM Band 3 (Red) Reflectance greater than 2 standard deviations from mean change between 1987 and 1990.
- Decrease less than two standard deviations from mean change or increase in Landsat TM Band 3 (Red) Reflectance between 1987 and 1990.

Figure 5. Spatial patterns of extreme change in Red Reflectance and TCB (1987 through 1990).

During this same time period, the areas that increased in brightness or decreased much less than the mean decrease in brightness for the study area (highlighted in red) appeared to occur in isolated areas of high productivity or vegetative cover. An increase in brightness, or a decrease much less than the mean decrease would generally indicate a decrease in vegetative cover or increase in exposed soils for these areas, but because these areas of extreme change occurred in areas of high cover, it is more likely that these extreme changes were due to differences in climatic conditions between the two dates. However, precipitation records indicate that precipitation before the 1990 date was significantly higher than precipitation before the 1987 date. Therefore, these areas of high productivity should have had more moisture available, especially in depression areas, and one would expect an increase, and not a decrease, in vegetative cover and vigor in these areas. It is probably more likely that a single precipitation event just before the 1987 image acquisition date caused a green-up of perennials and annuals and an increase in soil moisture, which may have caused these areas to appear significantly brighter in 1990. Areas where these extreme changes were most evident were the extreme western edge of the study area, extending south from Old Coe Lake in Maneuver Area 4B, and to a lesser extent, in Maneuver Area 4C. A second area where this type of change was evident was in the southeast corner of the study area, on the McGregor Range, directly east of Alvarado Tank. Other similar changes occurred in isolated areas of high cover throughout the study area.

Between 1990 and 1993, there was a very slight increase in mean brightness for both TCB (0.10) and Red Reflectance (10.84) for the entire study area. Figure 6 is a map of those areas of extreme change (+/- 2 s.d. from mean change) for TCB and Red Reflectance. Similar to the 1987 to 1990 evaluation, areas of extreme change occurred in primarily the same areas. However, the same areas that became less bright or less reflective between 1987 and 1990 seemed to increase in brightness and reflectivity between 1990 and 1993. Likewise, those areas that increased in brightness or reflectivity between 1987 and 1990 seemed to decrease in brightness and reflectivity between 1990 and 1993. Besides this reversal in direction of change, the only other notable difference between the two different time sequences appeared to be an increase in total area of extreme change on the McGregor Range from 1990 to 1993 relative to 1987 to 1990. Unlike 1987 to 1990, where there appeared to be a relatively equal amount of extreme increases and decreases, between 1990 and 1993, almost all of the extreme changes were increases in brightness. These extreme increases in brightness indicate a relative decrease in vegetative cover or vigor, which may have been the result of less antecedent precipitation before the 1993 acquisition date relative to the 1990 acquisition date.

Legend:

Decrease in Tasseled-Cap Brightness Index greater than 2 standard deviations from mean change between 1990 and 1993.

Increase in Tassled-Cap Brightness Index greater than 2 standard deviations from mean change between 1990 and 1993.

Legend:

Increase less than 2 standard deviations from mean change or decrease 2 in Landsat TM Band 3 (Red) Reflectance between 1990 and 1993.

Increase in Landsat TM Band 3 (Red) Reflectance greater than 2 standard deviations from mean change between 1990 and 1993.

Figure 6. Spatial patterns of extreme change in Red Reflectance and TCB (1990 through 1993).

Between 1987 and 1993, there was a decrease in mean brightness for both TCB (-4.72) and Red Reflectance (-12.57) for the entire study area. Figure 7 shows a map of those areas of extreme change (+/- 2 s.d. from mean change) for TCB and Red Reflectance. Spatial patterns of extreme change for this time period were very similar to those observed between 1990 and 1993. Again, most of the areas of extreme change were areas that either increased in brightness, or decreased, but much less than the mean decrease for the entire study area. Most of these

increases in brightness occurred in north-south oriented linear depressions that extend south from Old Coe Lake in Maneuver Area 4B, and in the southeastern corner of the study area, on McGregor Range, directly east of Alvarado Tank. In each of the time periods observed, there appeared to be an area of increasing brightness, or decreasing cover, in the southeastern corner of the study area, on McGregor Range. Between 1987 and 1993, the total area of increased brightness was the greatest for all time periods observed. Since this area of McGregor Range is not impacted by tracked and wheeled vehicles, it is more likely that the observed patterns of increasing brightness are due to natural changes rather than military impacts.

The spatial patterns of extreme change between different dates were identified by delineating those areas that changed beyond 2 standard deviations from mean change. By evaluating differences from the mean change, rather than the simple difference between two dates, those climatic effects that would have affected brightness values uniformly across the entire study area should have been minimized. However, the extreme changes that were observed were still most likely attributable to climatic factors, such as differences in soil moisture, or differences in vegetative growth, vigor, and greenness. The differences were simply more extreme in isolated areas of either high or low vegetative cover.

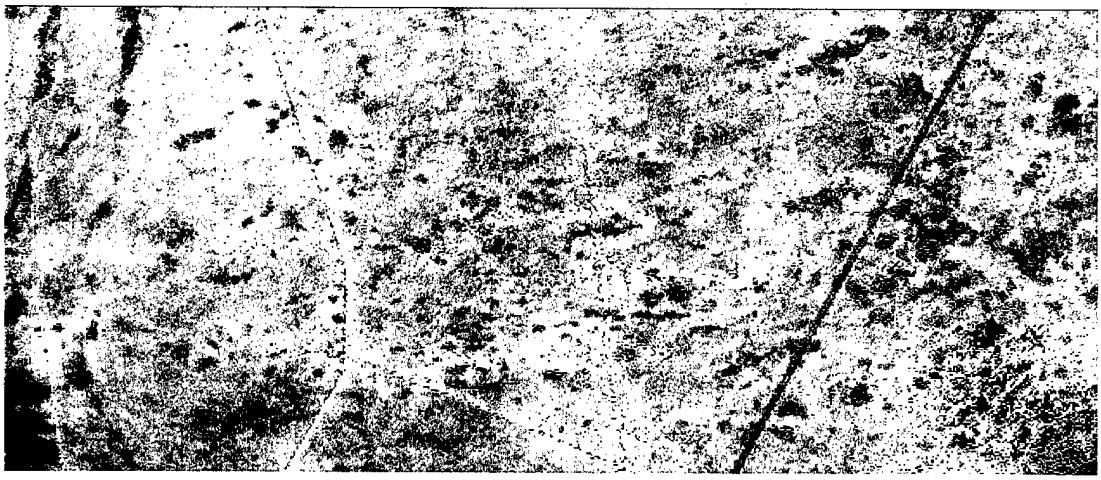

Legend:

- Decrease in Landsat TM Band 3 (Red) Reflectance greater than 2 standard deviations from mean change between 1987 and 1993.
- Decrease less than 2 standard deviations from mean change or an increase in Landsat TM Band 3 (Red) Reflectance between 1987 and 1993.

Legend:

- Decrease in Tasseled-Cap Brightness Index greater than 2 standard deviations from mean change between 1987 and 1993.
- Increase in Tassled-Cap Brightness Index greater than 2 standard deviations from mean change between 1987 and 1993.

Figure 7. Spatial patterns of extreme change in Red Reflectance and TCB (1987 through 1993).

6 Summary and Recommendations

Summary

The primary goal of this research was to assess relative, temporal trends in land condition using remotely sensed spectral indices for a specific study site at Fort Bliss, Texas. A secondary goal of this research was to observe spatial patterns of detected changes in land condition, and to compare trends and patterns for areas that have been impacted by military training with those that have not been impacted by the training mission.

Spectral brightness and greenness indices were calculated from temporal imagery and were used as a surrogate measure of the relative abundance of vegetative cover on the Earth's surface. Observations of trends in brightness and greenness indices over a 23-year period from 1972 through 1994 revealed considerable variations in brightness or reflectance of the study area. However, when analyzed in conjunction with precipitation data for the same time period, most variation in spectral indices could be related to natural variations in the amount of monthly and annual precipitation for the region. In most cases, large increases or decreases in spectral indices were probably the result of an increase in growth and vigor of both perennials and annuals during seasons of above normal precipitation, and conversely, a decrease in growth and vigor during drought periods. In addition, although extremes in brightness and greenness indices were observed for some individual image dates, spectral indices appeared to return to close to mean values after a relatively short period of time. This would seem to indicate that land condition tended to degrade or improve in response to short-term climate variations, or possibly anthropogenic disturbances such as military training, but there was no indication of permanent, long-term changes in land condition. In summary, the study area appeared to be resilient, with no clearly observable trends toward either long-term degradation or improvement.

Comparison of trends in spectral indices between impacted and unimpacted areas of the study site revealed a noticeable difference between the heavily impacted maneuver areas on the west side of Highway 54 and the McGregor Guided Missile Range on the east side of the highway. Brightness indices for the maneuver areas were consistently higher than brightness indices for McGregor Range, indicating that the maneuver areas most likely have less total vegetative

cover. However, the observed trends in brightness and greenness indices for both the East and West study areas were very similar. This indicated that the cause of these observed variations in trend was more likely attributable to climatic or phenological changes that occurred uniformly across the study area as opposed to military or other anthropogenic impact. If an increase in brightness provided some indication of a decrease in vegetative cover or increase in soil disturbance due to military impacts, there should have been an observable difference in response between the maneuver areas (West) and McGregor Range (East). This difference was not observed. The only exception to this observed trend was between 1992 and 1994, where differences between indices for the East and West decreased substantially.

Observations during the time period of this study do not provide enough data to conclude that observed differences between East and West can be attributed to military impact. The contrasting historical land uses between the maneuver areas and McGregor Range provide the most reasonable explanation as to why there is a considerable difference in spectral indices for the two areas. However, during the time period of this study, there has not been a significant increase or decrease in the difference between these two areas. The differences are probably the result of cumulative training impacts over a much longer time period. Comparison of trends in indices between an area of high and low vegetative cover within the maneuver areas revealed similar results. Again, there was a consistent difference in spectral indices for the two areas, but no significant variation in the difference between the two areas that would indicate that a change had actually occurred during the time period of this study.

Spatial patterns of change were variable across different temporal sequences, as expected. Different change detection techniques, when applied to the same temporal sequence, revealed similar patterns of change, which served to verify that detected changes in the imagery represented actual changes in land condition and cover on the ground. In most cases, areas of extreme change seemed to occur in depressions, or isolated areas of high productivity and vegetative cover, or in areas of extremely low vegetative cover or completely exposed soils. There was no indication that these areas of extreme change occurred in areas that were heavily impacted by tracked and wheeled vehicle maneuvers. Again, the extreme changes in spectral indices that were observed for these areas were most likely attributable to short-term changes in vegetative growth and vigor in response to short-term variations in the amount of rainfall and corresponding soil moisture.

Quantification of the abundance of vegetative cover with remotely sensed imagery is difficult and requires an empirical relationship between indices and

ground measurements for the purpose of calibration. Field measurements of cover were not available for calibration; therefore, only relative trends, rather than absolute changes in cover amounts, were assessed in this study. Even if ground observations of vegetative cover had been available, the archival imagery from which the spectral indices were derived was collected at a very coarse spatial resolution (80 m and 30 m). In arid environments such as Fort Bliss, where vegetative cover is sparse, a single pixel records the reflectance of a heterogeneous mixture of vegetative cover, including both live and standing dead material, litter, shadows, and significant areas of bare ground between plants. Therefore, because of this mixed spectral response, it would have been very difficult to calibrate spectral indices with ground measurements for the purpose of calibration and actual quantification of vegetative abundance.

Assessment of trends in vegetation and brightness indices calculated from temporal image data sets still provides a cost-effective method for monitoring *relative* trends in land condition. Documentation of historical trends in land condition may be useful at an upper management level for evaluating the effectiveness of historical resource management efforts, including Land Rehabilitation and Maintenance over long periods of time and across large geographic areas. Documentation may also be useful for identification of areas of extreme degradation, or "problem areas," where there is a continual trend toward degradation and no evidence of recovery. The ability to monitor vegetative cover dynamics of training lands may provide more information about land condition and carrying capacity of these lands than actual measurements of vegetative cover, structure, or pattern at any one time. Therefore, although the trends observed in this study provided only a relative, rather than absolute, measure of changing vegetative cover, they are still of great utility to installation land managers.

Recommendations

Archival remotely sensed imagery, and specifically, soil brightness and vegetation indices calculated from remotely sensed reflectance, provide installation land managers with the necessary tools to assess *relative* changes in general land condition at small scales, or across large geographic areas. Characterization and monitoring of *absolute* changes in vegetative cover requires detailed ecological field surveys that allow for empirical relationships between remotely sensed reflectance and ground-based cover measures. Alternatively, the use of spectral mixture models, which estimate the amount of cover based on a proportional amount of the total reflectance that originates from vegetative cover, could provide improved estimates of absolute change in vegetative cover. Higher spatial resolution imagery is also optimal for characterization of cover in arid envi-

ronments where vegetative cover is sparse and variable over very short distances.

Regardless of whether the intent is to monitor *relative* or *absolute* changes in vegetative cover on military lands, establishing cause and effect relationships requires not only detailed ecological field surveys, climate data, and higher spatial and spectral resolution imagery, but also detailed information on military training activities. Improved information on the spatial and temporal distribution and intensity of training and testing activities is required to establish relationships between military impact and observed patterns of change in land condition using combined remote sensing and field survey technologies. Collection of ecological data, as well as training data, is both costly and time consuming, especially for large installations such as Fort Bliss. Therefore, methods are required to scale up absolute estimates of vegetative cover derived from spectral mixture models and cover-radiance models to smaller scales or larger geographic regions for monitoring purposes. In the absence of reliable procedures for scaling between large scale observations at field sample sites and small scale observations of entire training areas or installations, temporal analysis of coarse resolution satellite imagery still provides a cost-effective method for *relative* characterization and monitoring of installation training lands.

References

Anderson, G.L., J.D. Hanson, and R.H. Haas. 1993. "Evaluating Landsat Thematic Mapper Derived Vegetation Indices for Estimating Above Ground Biomass on Semiarid Rangelands," *Remote Sensing of Environment*, Aug., vol. 45, n2, pp 165-175.

Boyd, W.E. 1986. "Correlation of Rangelands Brush Canopy Cover with Landsat MSS Data," *Journal of Range Management*," 39(3), pp 268-271.

Curran, P.J. 1980. "Multispectral Remote Sensing of Vegetation Amount," *Progress in Physical Geography*, 4:315-341.

Campbell, J.B. 1987. *Introduction to Remote Sensing*, Guilford Press, New York, NY.

ERDAS, 1993. *Field Guide*, Earth Resources Data Analysis Systems (ERDAS) Inc., Atlanta, GA.

Duncan, J., D. Stow, J. Franklin, and A. Hope. 1993. "Assessing the Relationship Between Spectral Vegetation Indices and Shrub Cover in the Jornada Basin, New Mexico," pp 3395-3416 in *International Journal of Remote Sensing*, Vol. 14, No. 18.

Frank, T. 1984. "The Effect of Change in Vegetation Cover and Erosion Patterns on Albedo and Texture of Landsat Images in a Semiarid Environment," *Annals of the Association of American Geographers*, 74(3), pp 393-407.

Fort Bliss Terrain Analysis. 1978. Map book. Topographic Engineering Center.

Graetz, R.D., and M.R. Gentle. 1982. "The Relationship Between Reflectance in the LANDSAT Wavebands and the Composition of an Australian Semi-Arid Shrub Rangeland," *Photogrammetric Engineering and Remote Sensing*, 11:1721-1730.

Huete, A.R. 1988. "A Soil-Adjusted Vegetation Index (SAVI)," *Remote Sensing of the Environment*, 25:295-309.

Kauth, R.J., P.F. Lambeck, W. Richardson, G.S. Thomas, and A.P. Pentland. 1978. "Feature Extraction Applied to Agricultural Crops As Seen by Landsat," *Proceedings of the Technical Sessions* Vol II, The LACIE Symposium. Oct 1978, NASA Johnson Space Center.

Lillesand, T.M., and R.W. Kiefer. 1987. *Remote Sensing and Image Interpretation*, John Wiley and Sons, New York, NY.

Markham, B.L., and J.L. Barker. 1986. "Landsat MSS and TM Post-Calibration Dynamic Ranges, Exoatmospheric Reflectances and At-Satellite Temperatures," EOSAT LANDSAT Technical Notes.

McDaniel, K.C., and R.H. Haas. 1982. "Assessing Mesquite-Grass Vegetation Condition from Landsat," *Photogrammetric Engineering and Remote Sensing*, Vol. 48, No. 3, pp 441-450.

Musick, H.B. 1984. "Assessment of Landsat Multispectral Scanner Spectral Indexes for Monitoring Arid Rangeland," pp 512-520 in *IEEE Transactions on Geoscience and Remote Sensing*, vol. GE-22, no. 6.

Musick, H.B. 1986. "Temporal Change of Landsat MSS Albedo Estimates in Arid Rangeland," *Remote Sensing of Environment*, 20:107-120.

Pickup, G., V.H. Chewings, and D.J. Nelson. 1993. Estimating Changes in Vegetative Cover over Time in Arid Rangelands Using Landsat MSS Data, *Remote Sensing of Environment*, 43:243-263.

Price, K.P., D.A. Pyke, and L. Mendes. 1992. "Shrub Dieback in a Semiarid Ecosystem: The Integration of Remote Sensing and Geographic Information Systems for Detecting Vegetation Change," *Photogrammetric Engineering and Remote Sensing*, Vol. 58, No. 4, pp 455-463.

Qi, J., A. Chehbouni, A.R. Huete, Y.H. Kerr, and S. Sorooshian. 1994. "A Modified Soil Adjusted Vegetation Index," *Remote Sensing of the Environment*, 48:119-126.

Richardson, A.J., and C.L. Wiegand. 1977. "Distinguishing Vegetation from Soil Background Information," *Photogrammetric Engineering and Remote Sensing*, 43:1541-1552.

Robinove, C.J., P.S. Chavez, D. Gehring, and R. Holmgren. 1981. "Arid Land Monitoring Using Landsat Albedo Difference Images," *Remote Sensing of the Environment*, 11:133-156.

Rondeaux, G., and M. Steven. 1996. "Optimization of Soil-Adjusted Vegetation Indices," *Remote Sensing of the Environment*, 55:95-107.

Rouse, J.W., R.H. Haas, J.A. Schell, D.W. Deering, and J.C. Harlan. 1973. "Monitoring vegetation systems in the great plains with ERTS," *Third ERTS Symposium*, NASA SP-351 I:309-317.

Scarpace, F.L., M. Mackenzie, N. Podger, R. Saleh, L. Seidl, M. Verhage, and P. Weiler. 1995. "Application of GIS and Remote Sensing for Resource Management in the Northern Chihuahuan Desert, an Environmental Monitoring Practicum," University of Wisconsin Environmental Remote Sensing Center.

Senseman, G.M., C.F. Bagley, and S.A. Tweddale. 1996. "Correlation of Rangeland Cover Measures to Satellite-Imagery-Derived Vegetation Indices," *Geocarto International*. 11(3):29-38.

Singh, A. 1989. "Digital Change Detection Techniques Using Remote Sensed Data," *International Journal of Remote Sensing*, 10, pp 989-1003.

Tazik, D.J., S.D. Warren, V.E. Diersing, R.B. Shaw, R.J. Brozka, C.F. Bagley, and W.R. Whitworth. 1992. *U.S. Army Land Condition-Trend Analysis (LCTA) Plot Inventory Field Methods.* Construction Engineering Research Laboratories (CERL) Technical Report N-92/03/ADA247931, U.S. Army CERL, Champaign, IL.

Tucker, C.J. 1979, "Red and Photographic Infrared Linear Combinations for Monitoring Vegetation," *Remote Sensing of the Environment*, 8:127-150.

Wu, X., and J.D. Westervelt. 1994. *Using Neural Networks to Correlate Satellite Imagery and Ground-truth Data.* USACERL Special Report (SR) EC-94/28/ADA285486. U.S. Army CERL.

Yool, S.R., M.J. Makaio, and J.M. Watts. 1987. "Techniques for Computer-Assisted Mapping of Rangeland Change," *Journal of Range Management*, 50(3):307-314.

Zhuang, H.C., M. Shapiro, and C.F. Bagley. 1993. "Relaxation Vegetative Index in Non-Linear Modeling of Ground Plant Cover by Satellite Remote-Sensing Data." *International Journal of Remote Sensing*. Vol. 14(18): 3447-3470.

Appendix A: Calibration Values

Digital Numbers extracted from a pond in Sunlake Park, El Paso, Texas.

MSS Images

Acq. Date:	Band 1	Band 2	Band 3	Band 4
09-06-72	13.906	10.171	8.588	13.221
12-23-72	17.546	15.868	15.160	13.883
10-20-74	15.011	15.962	13.527	9.605
11-25-74	16.821	14.787	14.906	13.120
09-30-76	12.735	13.457	15.688	15.025
09-29-78	12.015	12.604	13.008	12.983
12-26-80	11.983	11.009	10.862	8.310
06-28-82	11.451	*7.983	*7.129	*6.658
12-05-83	*10.559	9.587	9.165	9.033
10-28-84	13.491	11.484	10.581	9.474

TM Images

Acq. Date:	Band 1	Band 2	Band 3	Band 4	Band 5	Band 7
10-28-84	10.97	8.627	7.174	4.272	0.918	*0.086
08-15-86	*5.310	*3.358	*2.401	*1.443	*0.734	0.197
09-19-87	9.900	7.621	6.256	4.342	1.938	1.149
08-24-88	6.760	4.305	3.108	2.024	1.123	0.350
10-13-90	6.502	6.051	4.338	2.099	0.866	0.428
06-04-92	7.597	6.757	4.965	4.873	2.790	1.917
10-18-92	6.630	6.170	4.424	2.141	0.884	0.436
09-19-93	5.959	4.390	3.567	2.774	1.544	0.958
11-09-94	6.437	4.544	3.030	1.733	0.967	0.582

* an asterisk indicates lowest mean value for each band to subtract from other images.

Appendix B: Statistics and Index Values

ALBEDO

TM	Full	sd	min	max	East	sd	min	max	West	sd	min	max
94.11	14.494	1.032	5.298	35.471	14.527	1.151	5.298	35.471	14.488	0.994	8.474	34.240
93.9	14.316	1.032	6.846	19.707	14.207	1.099	8.293	19.219	14.344	1.008	7.605	19.707
92.10	13.701	0.984	6.207	21.206	13.597	1.058	7.455	19.003	13.731	0.960	7.541	21.206
92.6	12.181	1.135	6.319	18.900	11.219	0.967	6.319	16.665	12.438	1.031	6.778	18.900
90.10	13.838	1.297	5.073	25.672	13.061	1.463	5.690	18.949	14.053	1.156	6.200	25.672
88.8	14.221	1.257	6.261	21.755	13.646	1.447	6.630	20.013	14.377	1.151	6.678	21.755
87.9	12.443	1.073	5.359	18.794	11.833	1.170	5.559	18.794	12.608	0.978	6.203	18.771
86.8	11.907	0.988	5.696	17.819	11.455	1.137	5.950	16.049	12.030	0.903	5.988	17.819
84.10	13.633	1.461	4.170	19.963	12.940	1.651	4.170	19.715	13.820	1.340	5.361	19.637

TM	Low Cover	sd	min	max	High Cover	sd	min	max
94.11	15.009	0.948	9.341	34.240	14.627	0.997	9.341	34.240
93.9	15.163	0.937	9.028	19.349	14.584	1.128	9.028	19.349
92.10	14.614	0.883	9.010	18.172	14.063	1.063	9.010	18.172
92.6	13.501	0.956	8.226	17.917	13.014	1.054	8.226	17.917
90.10	15.033	1.026	7.484	20.211	14.409	1.236	7.484	20.211
88.8	15.040	1.027	8.385	20.275	14.517	1.161	8.385	20.275
87.9	13.233	0.898	6.799	17.092	12.797	0.998	6.799	17.092
86.8	12.549	0.809	7.328	16.658	12.138	0.913	7.328	16.658
84.10	14.385	1.314	7.151	19.385	14.110	1.204	7.151	19.385

MSS	Full	sd	min	max	East	sd	min	max	West	sd	min	max
84.10	18.474	1.410	8.796	23.620	17.725	1.552	10.446	23.483	18.683	1.291	8.796	23.620
83.12	10.698	0.605	5.841	14.219	10.575	0.732	6.178	14.219	10.734	0.558	5.841	13.369
82.6	20.600	0.981	14.542	27.551	20.859	1.199	14.542	27.551	20.532	0.898	14.671	25.017
80.12	21.502	1.423	11.753	28.042	21.357	1.772	11.844	28.042	21.542	1.304	11.935	27.340

78.9	16.931	1.155	6.754	22.648	16.566	1.419	7.217	22.648	17.037	1.043	6.754	21.116
76.9	18.347	1.368	7.904	25.551	18.847	1.519	9.428	25.551	18.214	1.287	7.904	23.254
74.11	17.080	1.300	5.416	22.815	17.672	1.448	8.425	22.815	16.922	1.201	5.416	22.459
74.10	18.742	1.302	6.826	24.685	18.508	1.494	6.882	23.259	18.810	1.227	6.826	24.685
72.12	30.306	2.536	7.120	40.606	31.233	2.558	12.918	38.333	30.061	2.459	7.120	40.606
72.9	25.225	1.639	10.332	32.295	25.785	1.681	13.876	30.576	25.077	1.586	10.332	32.295

MSS	Low Cover	sd	min	max	High Cover	sd	min	max
84.10	19.050	1.291	11.290	23.620	18.934	1.163	11.290	23.620
83.12	10.879	0.552	7.707	12.485	10.812	0.512	7.707	12.485
82.6	20.825	0.811	15.935	24.028	20.551	0.807	15.935	24.028
80.12	22.039	1.234	14.487	27.089	21.716	1.190	14.487	27.089
78.9	17.274	0.939	9.880	21.116	17.187	0.885	9.880	21.116
76.9	18.110	1.012	11.599	21.852	18.042	1.024	11.599	21.852
74.11	17.408	1.013	9.348	20.627	16.998	1.077	9.348	20.627
74.10	19.111	1.069	9.726	22.403	18.824	1.084	9.726	22.403
72.12	29.419	1.987	15.088	36.639	29.544	1.793	15.088	37.368
72.9	24.727	1.307	15.295	29.275	24.759	1.168	15.295	30.111

RED

TM	Full	sd	min	max	East	sd	min	max	West	sd	min	max
94.11	15.299	1.350	4.172	72.796	15.227	1.531	4.463	65.527	15.323	1.291	7.080	72.796
93.9	14.312	1.311	4.761	21.567	14.144	1.479	5.192	20.059	14.355	1.254	4.761	21.567
92.10	13.494	1.235	4.795	22.639	13.329	1.369	6.034	19.913	13.540	1.189	5.787	22.639
92.6	12.154	1.425	4.620	20.897	11.007	1.271	4.620	17.450	12.459	1.298	4.620	20.897
90.10	13.513	1.633	3.291	23.218	12.584	1.892	3.291	19.573	13.771	1.449	3.534	23.218
88.8	14.446	1.574	4.229	23.707	13.760	1.852	4.229	21.177	14.632	1.431	4.987	23.707

87.9	17.025	1.959	4.011	29.004	15.929	2.135	4.873	28.358	17.324	1.792	4.011	29.004
86.8	11.890	1.236	3.873	19.157	11.351	1.457	3.873	16.973	12.036	1.123	4.667	19.157
84.10	15.076	2.116	2.757	23.884	14.161	2.421	2.757	23.356	15.323	1.948	3.549	23.884

TM	Low Cover	sd	min	max	High Cover	sd	min	max
94.11	15.840	1.261	7.952	72.796	15.513	1.224	7.952	72.796
93.9	15.163	1.196	5.839	20.921	14.634	1.285	5.839	20.921
92.10	14.495	1.100	7.769	19.170	13.935	1.239	7.769	19.170
92.6	13.673	1.209	6.535	19.174	13.170	1.273	6.535	19.174
90.10	14.839	1.310	4.263	21.517	14.235	1.452	4.263	21.517
88.8	15.234	1.260	6.758	21.683	14.769	1.327	6.758	21.683
87.9	18.186	1.645	6.597	25.988	17.615	1.691	6.597	25.988
86.8	12.508	0.993	5.858	17.569	12.142	1.044	5.858	17.569
84.10	15.870	1.855	4.605	22.828	15.723	1.671	4.605	23.356

MSS	Full	sd	min	max	East	sd	min	max	West	sd	min	max
84.10	17.114	1.704	5.860	23.391	16.312	1.897	7.041	22.633	17.338	1.575	5.860	23.391
83.12	18.077	1.452	6.954	28.192	17.706	1.738	8.069	28.192	18.185	1.339	7.052	24.831
82.6	21.942	1.165	14.570	29.860	22.250	1.397	14.909	29.860	21.860	1.077	14.570	26.936
80.12	18.541	1.427	9.068	25.174	18.421	1.771	9.608	25.174	18.574	1.311	9.068	23.746
78.9	16.607	1.550	2.704	23.203	16.299	1.842	4.088	23.203	16.697	1.442	2.704	22.024
76.9	18.712	1.682	5.333	27.722	19.148	1.808	6.574	27.722	18.593	1.622	5.333	24.683
74.11	16.024	1.409	4.109	21.648	16.815	1.509	9.837	21.648	15.812	1.298	4.109	21.386
74.10	17.103	1.557	4.433	24.323	16.707	1.776	6.075	23.180	17.219	1.465	4.433	24.323
72.12	19.542	1.910	3.115	28.115	20.161	1.883	8.115	26.115	19.378	1.877	3.115	28.115
72.9	25.737	1.887	9.332	34.625	26.357	1.860	14.510	32.305	25.573	1.853	9.332	34.625

MSS	Low Cover	sd	min	max	High Cover	sd	min	max
84.10	17.749	1.556	8.284	23.391	17.640	1.414	8.284	23.391

83.12	18.482	1.310	11.177	21.934	18.399	1.221	11.177	22.167
82.6	22.103	1.019	16.017	25.822	21.891	0.956	16.017	25.822
80.12	18.969	1.247	11.827	23.746	18.751	1.174	11.827	23.746
78.9	16.860	1.304	6.556	21.704	16.789	1.231	6.556	21.704
76.9	18.337	1.278	9.314	22.878	18.384	1.304	9.314	22.878
74.11	16.266	1.116	8.591	19.799	15.865	1.181	8.591	19.799
74.10	17.576	1.265	7.376	22.076	17.297	1.305	7.376	22.076
72.12	18.727	1.491	9.115	24.115	18.906	1.414	9.115	25.115
72.9	24.922	1.458	15.017	30.052	25.102	1.382	15.017	31.767

TCAP BRIGHT

TM	Full	sd	min	max	East	sd	min	max	West	sd	min	max
94.11	53.924	2.766	24.091	103.658	54.284	3.123	25.829	103.246	53.839	2.639	35.797	103.658
93.9	53.081	2.747	30.178	67.541	53.208	3.104	30.394	65.456	53.042	2.632	33.242	67.541
92.10	51.955	2.689	28.509	70.862	51.909	3.040	32.762	64.296	51.972	2.579	33.978	70.862
92.6	39.024	3.173	20.236	56.587	36.348	2.959	20.236	48.648	39.739	2.814	21.754	56.587
90.10	52.995	3.491	25.154	72.472	51.128	4.184	27.582	65.613	53.517	3.072	26.827	72.472
88.8	52.523	3.485	20.282	70.061	51.293	4.224	20.282	66.678	52.861	3.168	25.655	70.061
87.9	57.812	3.715	30.710	79.225	55.898	4.101	32.922	78.159	58.335	3.411	34.492	79.225
86.8	44.635	2.737	19.336	58.397	43.667	3.322	19.336	54.753	44.900	2.486	22.721	58.397
84.10	53.912	4.498	22.288	71.951	51.976	5.288	22.288	70.426	54.442	4.084	22.326	71.388

TM	Low Cover	sd	min	max	High Cover	sd	min	max
94.11	54.551	2.491	38.422	103.658	54.031	2.402	38.422	103.658
93.9	54.495	2.481	36.858	64.948	53.484	2.614	36.858	64.948
92.10	53.785	2.399	38.053	62.796	52.764	2.535	38.053	62.796
92.6	42.157	2.621	26.163	52.958	41.309	2.609	26.163	52.958
90.10	55.465	2.749	34.374	68.475	54.321	2.958	34.374	68.475

88.8	53.859	2.706	34.366	66.159	52.989	2.774	34.366	66.159
87.9	59.831	3.102	37.929	72.694	58.793	3.167	37.929	72.694
86.8	45.682	2.132	30.388	55.335	44.998	2.182	30.388	55.335
84.10	54.970	3.902	33.475	69.069	55.042	3.428	33.475	69.069

MSS	Full	sd	min	max	East	sd	min	max	West	sd	min	max
84.10	36.462	2.885	16.343	46.605	34.969	3.205	19.910	46.570	36.881	2.640	16.343	46.605
83.12	37.984	2.459	17.820	52.441	37.466	2.970	19.176	52.441	38.138	2.266	17.820	48.430
82.6	41.509	2.035	28.574	55.491	42.081	2.436	28.574	55.491	41.357	1.878	29.147	50.497
80.12	36.463	2.535	18.758	47.516	36.206	3.179	19.462	47.516	36.535	2.315	18.758	46.439
78.9	32.774	2.335	11.732	43.177	32.065	2.877	12.822	43.177	32.980	2.106	11.732	40.650
76.9	35.585	2.797	14.729	49.550	36.631	3.048	17.808	49.550	35.305	2.646	14.729	45.123
74.11	32.625	2.614	9.011	43.838	33.837	2.920	13.677	43.838	32.301	2.407	9.011	43.136
74.10	37.312	2.697	11.359	49.225	36.872	3.113	11.359	46.824	37.441	2.538	12.381	49.225
72.12	39.264	3.364	8.510	52.514	40.531	3.372	16.287	49.628	38.928	3.264	8.510	52.514
72.9	49.454	3.352	19.006	62.924	50.720	3.361	26.699	59.798	49.118	3.251	19.006	62.924

MSS	Low Cover	sd	min	max	High Cover	sd	min	max
84.10	37.458	2.609	21.707	46.605	37.354	2.345	21.707	46.605
83.12	38.638	2.214	25.607	44.874	38.467	2.049	25.607	45.001
82.6	41.759	1.659	31.405	48.011	41.328	1.602	31.405	48.011
80.12	37.350	2.180	23.522	46.380	36.846	2.083	23.522	46.380
78.9	33.276	1.850	18.514	40.548	33.239	1.765	18.514	40.548
76.9	34.925	2.014	21.969	42.141	34.913	2.072	21.969	42.141
74.11	33.070	2.010	16.670	39.171	32.395	2.080	16.670	39.171
74.10	37.895	2.182	18.844	44.193	37.437	2.192	18.844	44.193
72.12	38.025	2.618	19.087	47.494	38.228	2.374	19.087	48.359
72.9	48.210	2.601	29.330	57.348	48.413	2.358	29.330	59.040

NIR

TM	Full	sd	min	max	East	sd	min	max	West	sd	min	max
94.11	24.322	1.988	0.653	110.353	24.734	2.179	9.394	109.479	24.212	1.901	0.653	110.353
93.9	24.774	1.641	10.055	32.399	24.800	1.736	11.674	31.104	24.765	1.610	11.674	32.399
92.10	24.921	1.652	10.164	35.494	24.697	1.852	12.026	32.514	24.986	1.582	12.399	35.494
92.6	22.292	1.847	10.187	31.555	20.694	1.759	11.054	27.513	22.721	1.612	10.187	31.555
90.10	25.109	2.114	7.438	57.844	23.630	2.494	9.629	32.276	25.519	1.791	7.438	57.844
88.8	23.599	2.145	2.141	34.839	22.403	2.485	2.141	31.797	23.926	1.915	6.703	34.839
87.9	27.690	2.201	9.782	38.279	26.376	2.456	10.753	37.956	28.047	1.971	12.696	38.279
86.8	18.973	1.684	2.136	27.793	18.033	1.952	2.136	24.809	19.230	1.504	4.224	27.793
84.10	25.322	2.428	0.806	35.738	24.150	2.837	0.806	33.753	25.639	2.189	1.203	35.341

TM	Low Cover	sd	min	max	High Cover	sd	min	max
94.11	24.619	1.734	12.454	110.353	24.296	1.715	12.454	110.353
93.9	25.671	1.456	13.941	31.104	25.069	1.574	13.941	31.104
92.10	25.986	1.357	16.124	31.024	25.533	1.375	16.124	31.396
92.6	23.864	1.423	14.230	30.112	23.537	1.393	14.230	30.112
90.10	26.350	1.580	15.474	33.372	25.801	1.670	15.474	33.372
88.8	24.564	1.662	12.406	31.797	24.093	1.696	12.406	31.797
87.9	29.065	1.814	12.696	35.689	28.421	1.901	12.696	35.689
86.8	19.729	1.312	10.191	25.406	19.360	1.336	10.191	25.406
84.10	26.072	2.023	15.096	33.753	26.024	1.838	15.096	33.753

MSS	Full	sd	min	max	East	sd	min	max	West	sd	min	max
84.10	23.714	1.631	9.164	30.720	22.995	1.810	9.164	29.052	23.917	1.513	10.890	30.720
83.12	24.952	1.637	11.818	32.907	24.765	1.892	11.818	32.907	25.011	1.546	11.943	31.104
82.6	23.762	1.185	15.850	30.067	24.118	1.317	15.850	30.067	23.668	1.122	17.221	27.782
80.12	22.214	1.575	11.364	28.717	22.055	1.902	11.364	28.717	22.259	1.464	12.657	28.343

78.9	20.152	1.391	4.845	25.451	19.644	1.691	4.845	25.166	20.302	1.246	9.223	25.451
76.9	20.116	1.667	6.939	27.911	20.987	1.785	6.939	27.911	19.883	1.544	8.444	25.390
74.11	24.267	2.125	-0.964	32.844	25.091	2.498	-0.964	32.844	24.045	1.936	2.107	31.120
74.10	29.709	2.191	2.329	37.011	29.778	2.616	2.329	37.011	29.694	2.041	5.011	35.984
72.12	29.828	2.664	5.775	40.775	31.005	2.628	5.775	38.775	29.516	2.564	7.775	40.775
72.9	30.989	2.650	6.502	41.580	32.171	2.613	6.502	39.720	30.675	2.549	9.259	41.580

MSS	Low Cover	sd	min	max	High Cover	sd	min	max
84.10	23.922	1.497	14.880	28.518	24.075	1.372	14.880	28.518
83.12	25.184	1.504	17.494	30.237	25.167	1.408	17.494	30.237
82.6	23.678	0.908	18.397	26.718	23.544	0.875	18.397	26.718
80.12	22.717	1.401	15.179	27.941	22.420	1.350	15.179	27.941
78.9	20.274	1.024	13.200	24.299	20.489	1.071	13.200	24.575
76.9	19.467	1.083	11.847	23.173	19.560	1.175	11.847	24.598
74.11	24.353	1.626	10.841	29.425	24.040	1.574	10.841	29.425
74.10	29.715	1.718	16.000	34.309	29.578	1.654	16.000	34.309
72.12	28.783	2.094	12.775	34.775	29.092	1.964	12.775	35.775
72.9	29.939	2.080	13.778	36.268	30.246	1.952	13.778	36.444

SAVI

TM	Full	sd	min	max	East	sd	min	max	West	sd	min	max
94.11	0.366	0.030	-1.428	1.231	0.383	0.033	-0.699	1.222	0.361	0.028	-1.428	1.231
93.9	0.431	0.031	-0.237	0.968	0.441	0.042	-0.237	0.968	0.428	0.027	0.306	0.910
92.10	0.478	0.028	0.357	0.716	0.481	0.028	0.370	0.716	0.478	0.028	0.357	0.692
92.6	0.473	0.037	0.318	0.983	0.490	0.040	0.318	0.983	0.469	0.035	0.319	0.806
90.10	0.484	0.041	-0.431	1.290	0.493	0.047	0.380	1.151	0.482	0.038	-0.431	1.290
88.8	0.387	0.031	-0.888	1.034	0.385	0.046	-0.888	1.034	0.388	0.026	-0.369	0.742

87.9	0.386	0.041	0.210	1.109	0.400	0.046	0.225	0.924	0.382	0.039	0.210	1.109
86.8	0.368	0.029	-0.799	0.969	0.364	0.042	-0.799	0.969	0.369	0.024	-0.565	0.696
84.10	0.412	0.059	-1.352	1.074	0.427	0.079	-1.352	1.038	0.407	0.051	-1.307	1.074

TM	Low Cover	sd	min	max	High Cover	sd	min	max
94.11	0.349	0.025	-0.788	1.169	0.355	0.025	-0.788	1.211
93.9	0.414	0.028	0.306	0.910	0.423	0.027	0.306	0.910
92.10	0.457	0.026	0.362	0.651	0.473	0.033	0.362	0.690
92.6	0.437	0.029	0.327	0.699	0.454	0.036	0.327	0.699
90.10	0.450	0.032	0.272	0.982	0.466	0.036	0.272	0.982
88.8	0.377	0.021	0.285	0.567	0.386	0.024	0.285	0.567
87.9	0.372	0.036	0.217	0.884	0.379	0.034	0.217	0.884
86.8	0.359	0.020	0.274	0.523	0.367	0.022	0.274	0.523
84.10	0.395	0.044	0.108	0.964	0.400	0.040	0.108	0.964

MSS	Full	sd	min	max	East	sd	min	max	West	sd	min	max
84.10	0.262	0.049	-0.458	0.678	0.275	0.058	-0.458	0.644	0.258	0.046	-0.173	0.678
83.12	0.257	0.040	-0.030	0.535	0.268	0.043	-0.008	0.470	0.254	0.039	-0.030	0.499
82.6	0.064	0.023	-0.030	0.238	0.065	0.023	-0.030	0.167	0.064	0.022	-0.027	0.238
80.12	0.145	0.032	0.017	0.375	0.145	0.035	0.027	0.375	0.145	0.031	0.017	0.335
78.9	0.156	0.054	-0.364	1.027	0.151	0.052	-0.364	0.740	0.158	0.055	-0.002	1.027
76.9	0.059	0.039	-0.390	0.556	0.074	0.041	-0.390	0.556	0.055	0.038	-0.087	0.550
74.11	0.328	0.059	-1.795	0.656	0.314	0.088	-1.795	0.519	0.331	0.048	-1.127	0.656
74.10	0.434	0.060	-1.095	0.944	0.452	0.078	-1.095	0.715	0.428	0.053	-0.897	0.944
72.12	0.336	0.051	-0.707	0.860	0.341	0.054	-0.707	0.550	0.334	0.050	-0.017	0.860
72.9	0.148	0.045	-0.846	0.347	0.159	0.048	-0.846	0.318	0.145	0.043	-0.290	0.347

MSS	Low Cover	sd	min	max	High Cover	sd	min	max
84.10	0.239	0.042	0.101	0.584	0.249	0.041	0.096	0.584

83.12	0.247	0.038	0.121	0.434	0.250	0.036	0.121	0.434
82.6	0.056	0.022	-0.027	0.163	0.059	0.022	-0.027	0.163
80.12	0.145	0.030	0.041	0.246	0.143	0.030	0.041	0.246
78.9	0.149	0.047	0.001	0.531	0.160	0.046	0.001	0.531
76.9	0.049	0.036	-0.074	0.288	0.050	0.034	-0.074	0.288
74.11	0.319	0.042	0.031	0.504	0.329	0.043	0.031	0.504
74.10	0.413	0.042	0.268	0.718	0.422	0.044	0.268	0.718
72.12	0.340	0.051	0.029	0.526	0.341	0.048	0.029	0.526
72.9	0.147	0.044	-0.145	0.310	0.149	0.042	-0.145	0.310

MSAVI2

TM	Full	sd	min	max	East	sd	min	max	West	sd	min	max
94.11	0.366	0.029	-4.206	0.862	0.380	0.029	-1.452	0.859	0.362	0.028	-4.206	0.862
93.9	0.418	0.024	-0.330	0.752	0.426	0.031	-0.330	0.752	0.416	0.021	0.316	0.722
92.10	0.454	0.020	0.359	0.614	0.456	0.020	0.370	0.614	0.454	0.020	0.359	0.600
92.6	0.450	0.028	0.326	0.759	0.463	0.029	0.326	0.759	0.447	0.026	0.327	0.668
90.10	0.458	0.029	-0.674	0.888	0.465	0.033	0.378	0.837	0.457	0.027	-0.674	0.888
88.8	0.384	0.030	-1.688	0.784	0.381	0.052	-1.688	0.784	0.384	0.021	-0.549	0.630
87.9	0.382	0.032	0.228	0.818	0.393	0.036	0.242	0.730	0.379	0.030	0.228	0.818
86.8	0.368	0.028	-1.411	0.755	0.365	0.046	-1.411	0.755	0.369	0.020	-0.927	0.603
84.10	0.402	0.057	-3.548	0.794	0.410	0.097	-3.548	0.794	0.400	0.041	-2.857	0.781

TM	Low Cover	sd	min	max	High Cover	sd	min	max
94.11	0.352	0.026	-1.797	0.837	0.357	0.024	-1.797	0.855
93.9	0.405	0.021	0.316	0.722	0.412	0.021	0.316	0.722
92.10	0.438	0.019	0.363	0.574	0.450	0.024	0.363	0.598
92.6	0.423	0.022	0.334	0.605	0.436	0.027	0.334	0.605

90.10	0.433	0.023	0.286	0.760	0.445	0.026	0.286	0.760
88.8	0.376	0.017	0.298	0.519	0.383	0.019	0.298	0.519
87.9	0.371	0.029	0.235	0.708	0.377	0.027	0.235	0.708
86.8	0.361	0.016	0.287	0.488	0.367	0.018	0.287	0.488
84.10	0.388	0.034	0.125	0.750	0.393	0.030	0.125	0.750

MSS	Full	sd	min	max	East	sd	min	max	West	sd	min	max
84.10	0.056	0.037	-0.329	0.317	0.066	0.041	-0.329	0.317	0.053	0.035	-0.207	0.312
83.12	0.094	0.035	-0.294	0.294	0.099	0.036	-0.184	0.288	0.092	0.034	-0.294	0.294
82.6	-0.008	0.024	-0.117	0.092	-0.008	0.025	-0.106	0.088	-0.007	0.024	-0.117	0.092
80.12	0.039	0.039	-0.132	0.604	0.040	0.042	-0.127	0.300	0.039	0.038	-0.132	0.604
78.9	0.062	0.039	-0.376	0.325	0.060	0.040	-0.376	0.325	0.063	0.038	-0.104	0.322
76.9	-0.017	0.039	-0.489	0.241	-0.009	0.040	-0.489	0.199	-0.019	0.039	-0.190	0.241
74.11	0.266	0.055	-4.069	0.508	0.262	0.096	-4.069	0.449	0.267	0.037	-1.090	0.508
74.10	0.288	0.042	-1.886	0.571	0.294	0.065	-1.886	0.424	0.286	0.034	-1.088	0.571
72.12	0.275	0.042	-0.636	0.649	0.275	0.043	-0.636	0.487	0.276	0.041	0.044	0.649
72.9	0.075	0.046	-1.396	0.308	0.082	0.049	-1.396	0.222	0.073	0.044	-0.421	0.308

MSS	Low Cover	sd	min	max	High Cover	sd	min	max
84.10	0.045	0.033	-0.105	0.187	0.049	0.033	-0.121	0.187
83.12	0.090	0.034	-0.017	0.242	0.090	0.033	-0.030	0.242
82.6	-0.009	0.025	-0.107	0.073	-0.009	0.024	-0.107	0.073
80.12	0.038	0.036	-0.096	0.234	0.037	0.036	-0.108	0.234
78.9	0.060	0.037	-0.066	0.205	0.064	0.037	-0.073	0.205
76.9	-0.023	0.038	-0.178	0.173	-0.022	0.038	-0.178	0.173
74.11	0.266	0.033	0.152	0.429	0.266	0.034	0.123	0.429
74.10	0.284	0.030	0.164	0.428	0.285	0.030	0.164	0.428
72.12	0.278	0.042	0.044	0.432	0.280	0.041	0.044	0.432
72.9	0.071	0.045	-0.228	0.210	0.075	0.043	-0.228	0.210

NDVI

TM	Full	sd	min	max	East	sd	min	max	West	sd	min	max
94.11	0.228	0.019	-0.913	0.759	0.238	0.020	-0.432	0.753	0.225	0.017	-0.913	0.759
93.9	0.269	0.020	-0.149	0.607	0.275	0.026	-0.149	0.607	0.267	0.017	0.190	0.571
92.10	0.298	0.018	0.221	0.451	0.300	0.018	0.230	0.451	0.298	0.018	0.221	0.436
92.6	0.296	0.024	0.198	0.618	0.307	0.026	0.198	0.618	0.293	0.022	0.198	0.510
90.10	0.302	0.026	-0.273	0.799	0.308	0.030	0.236	0.724	0.300	0.024	-0.273	0.799
88.8	0.241	0.020	-0.579	0.651	0.240	0.029	-0.579	0.651	0.242	0.016	-0.234	0.466
87.9	0.240	0.026	0.130	0.696	0.249	0.029	0.139	0.580	0.238	0.025	0.130	0.696
86.8	0.230	0.018	-0.525	0.613	0.228	0.027	-0.525	0.613	0.231	0.015	-0.363	0.440
84.10	0.256	0.037	-0.871	0.663	0.264	0.050	-0.871	0.663	0.254	0.032	-0.788	0.646

TM	Low Cover	sd	min	max	High Cover	sd	min	max
94.11	0.217	0.016	-0.487	0.721	0.221	0.016	-0.487	0.747
93.9	0.258	0.017	0.190	0.571	0.264	0.017	0.190	0.571
92.10	0.285	0.016	0.225	0.409	0.295	0.021	0.225	0.432
92.6	0.272	0.018	0.203	0.441	0.284	0.023	0.203	0.441
90.10	0.280	0.020	0.170	0.619	0.290	0.023	0.170	0.619
88.8	0.235	0.014	0.177	0.358	0.241	0.015	0.177	0.358
87.9	0.231	0.023	0.135	0.554	0.236	0.021	0.135	0.554
86.8	0.224	0.013	0.171	0.332	0.230	0.014	0.171	0.332
84.10	0.245	0.027	0.068	0.606	0.248	0.025	0.068	0.606

MSS	Full	sd	min	max	East	sd	min	max	West	sd	min	max
84.10	0.134	0.025	-0.171	0.356	0.137	0.028	-0.171	0.339	0.133	0.024	-0.011	0.356
83.12	0.111	0.024	-0.017	0.280	0.114	0.026	-0.006	0.239	0.110	0.023	-0.017	0.253
82.6	0.044	0.014	-0.009	0.128	0.044	0.014	-0.004	0.099	0.043	0.013	-0.006	0.128
80.12	0.070	0.021	-0.367	0.150	0.069	0.022	-0.016	0.150	0.070	0.020	-0.367	0.147

78.9	0.065	0.030	-0.151	0.559	0.063	0.029	-0.151	0.342	0.065	0.030	-0.024	0.559
76.9	0.045	0.022	-0.067	0.264	0.050	0.022	-0.036	0.247	0.043	0.022	-0.067	0.264
74.11	0.049	0.031	-0.551	0.161	0.042	0.037	-0.551	0.155	0.051	0.029	-0.401	0.161
74.10	0.104	0.030	-0.366	0.390	0.111	0.034	-0.366	0.255	0.102	0.029	-0.218	0.390
72.12	0.047	0.031	-0.205	0.257	0.052	0.031	-0.205	0.167	0.046	0.030	-0.148	0.257
72.9	0.052	0.021	-0.103	0.159	0.055	0.022	-0.103	0.131	0.051	0.021	-0.079	0.159

MSS	Low Cover	sd	min	max	High Cover	sd	min	max
84.10	0.125	0.022	0.033	0.273	0.130	0.022	0.031	0.273
83.12	0.106	0.023	0.034	0.218	0.108	0.022	0.034	0.218
82.6	0.039	0.013	-0.005	0.101	0.041	0.013	-0.005	0.101
80.12	0.070	0.019	-0.020	0.146	0.070	0.019	-0.020	0.146
78.9	0.061	0.026	-0.024	0.277	0.066	0.025	-0.024	0.277
76.9	0.042	0.021	-0.027	0.180	0.042	0.020	-0.027	0.180
74.11	0.044	0.026	-0.104	0.137	0.050	0.028	-0.104	0.161
74.10	0.093	0.025	0.004	0.240	0.098	0.025	0.004	0.240
72.12	0.049	0.031	-0.060	0.154	0.048	0.030	-0.060	0.154
72.9	0.053	0.022	-0.015	0.125	0.053	0.021	-0.017	0.125

TCAP GREEN

TM	Full	sd	min	max	East	sd	min	max	West	sd	min	max
94.11	1.320	0.809	-30.998	62.194	1.680	0.886	-25.413	62.012	1.222	0.761	-30.998	62.194
93.9	2.063	0.503	-7.278	10.224	2.224	0.610	-7.278	10.224	2.020	0.460	-0.473	9.819
92.10	3.200	0.480	-0.388	5.615	3.147	0.409	0.031	5.202	3.217	0.496	-0.388	5.615
92.6	2.995	0.580	-0.595	9.305	3.018	0.634	-0.595	9.305	2.992	0.563	-0.405	6.413
90.10	3.122	0.551	-7.903	33.182	2.907	0.463	0.401	11.386	3.180	0.559	-7.903	33.182
88.8	1.225	0.482	-8.314	8.915	0.946	0.509	-8.314	8.915	1.302	0.446	-7.137	5.467
87.9	2.407	0.649	-1.241	10.689	2.410	0.728	-1.241	7.655	2.406	0.624	-0.976	10.689
86.8	0.362	0.378	-7.182	6.396	0.143	0.397	-7.123	6.396	0.423	0.350	-7.182	3.691
84.10	2.763	0.629	-12.069	9.826	2.798	0.743	-12.069	9.826	2.753	0.593	-10.664	9.615

TM	Low Cover	sd	min	max	High Cover	sd	min	max
94.11	0.947	0.672	-30.002	61.204	1.121	0.714	-30.002	62.194
93.9	1.789	0.446	0.080	7.370	1.968	0.478	0.080	7.370
92.10	2.927	0.422	0.475	4.944	3.240	0.577	0.475	5.615
92.6	2.492	0.454	0.816	4.510	2.855	0.643	0.816	5.051
90.10	2.598	0.435	-0.924	9.322	2.906	0.575	-0.924	9.322
88.8	1.060	0.386	-0.945	3.449	1.286	0.481	-0.945	3.449
87.9	2.195	0.677	-0.976	8.727	2.398	0.656	-0.976	8.727
86.8	0.232	0.303	-1.341	1.815	0.410	0.378	-1.341	1.861
84.10	2.495	0.559	-2.571	8.165	2.680	0.576	-2.571	8.165

MSS	Full	sd	min	max	East	sd	min	max	West	sd	min	max
84.10	6.701	0.773	-5.688	11.024	6.590	0.867	-5.688	11.024	6.734	0.741	-1.087	10.378
83.12	6.227	0.796	1.183	10.838	6.263	0.846	1.826	10.838	6.220	0.780	1.183	9.780
82.6	3.531	0.587	0.865	5.731	3.647	0.582	1.277	5.682	3.501	0.581	0.976	5.731
80.12	4.368	0.693	-3.122	7.260	4.307	0.764	0.815	7.091	4.385	0.669	-3.122	7.260

78.9	3.703	0.714	-2.461	11.691	3.546	0.691	-2.461	6.637	3.750	0.712	0.922	11.691
76.9	2.803	0.701	-2.494	6.107	3.197	0.729	-2.494	6.107	2.700	0.652	-1.194	5.338
74.11	5.074	1.017	-10.493	8.566	5.155	1.220	-10.493	8.422	5.052	0.945	-7.910	8.566
74.10	8.103	1.120	-10.336	13.798	8.355	1.290	-10.336	11.847	8.033	1.056	-7.626	13.798
72.12	6.687	1.216	-6.232	11.384	7.236	1.224	-6.232	11.384	6.539	1.165	-1.292	10.574
72.9	5.956	1.181	-6.944	10.593	6.507	1.186	-6.944	10.593	5.807	1.129	-1.990	9.738

MSS	Low Cover	sd	min	max	High Cover	sd	min	max
84.10	6.393	0.697	3.114	9.346	6.665	0.761	3.114	9.346
83.12	6.106	0.753	3.778	9.128	6.228	0.743	3.778	9.128
82.6	3.199	0.475	1.670	4.945	3.334	0.505	1.670	5.211
80.12	4.433	0.647	1.694	7.207	4.410	0.636	1.694	7.207
78.9	3.477	0.637	1.287	6.475	3.785	0.734	1.287	6.475
76.9	2.415	0.568	0.314	4.252	2.556	0.601	0.314	4.971
74.11	4.792	0.789	-0.769	7.732	4.965	0.815	-0.769	7.732
74.10	7.695	0.842	3.866	10.755	7.880	0.867	3.866	10.755
72.12	6.252	1.068	0.339	9.837	6.452	1.054	0.339	9.837
72.9	5.519	1.033	-0.418	8.820	5.719	1.022	-0.418	9.009

CERL Distribution

Chief of Engineers
ATTN: CEHEC-IM-LH (2)

Directorate of Environment (2)
Fort Bliss, TX

Engineer Research and Development Center (Libraries)
ATTN: ERDC, Vicksburg, MS
ATTN: Cold Regions Research, Hanover, NH
ATTN: Topographic Engineering Center, Alexandria, VA

Defense Tech Info Center 22304
ATTN: DTIC-O

8
3/01

REPORT DOCUMENTATION PAGE

Form Approved
OMB No. 0704-0188

Public reporting burden for this collection of information is estimated to average 1 hour per response, including the time for reviewing instructions, searching existing data sources, gathering and maintaining the data needed, and completing and reviewing this collection of information. Send comments regarding this burden estimate or any other aspect of this collection of information, including suggestions for reducing this burden to Department of Defense, Washington Headquarters Services, Directorate for Information Operations and Reports (0704-0188), 1215 Jefferson Davis Highway, Suite 1204, Arlington, VA 22202-4302. Respondents should be aware that notwithstanding any other provision of law, no person shall be subject to any penalty for failing to comply with a collection of information if it does not display a currently valid OMB control number. PLEASE DO NOT RETURN YOUR FORM TO THE ABOVE ADDRESS.

1. REPORT DATE (DD-MM-YYYY)	2. REPORT TYPE	3. DATES COVERED (From - To)
04-2001	Final	

4. TITLE AND SUBTITLE
Historical Analysis of Land Cover/Condition Trends at Fort Bliss, Texas, Using Remotely Sensed Imagery

5a. CONTRACT NUMBER

5b. GRANT NUMBER

5c. PROGRAM ELEMENT NUMBER

6. AUTHOR(S)
Scott Tweddale

5d. PROJECT NUMBER
MIPR

5e. TASK NUMBER
96-08

5f. WORK UNIT NUMBER

7. PERFORMING ORGANIZATION NAME(S) AND ADDRESS(ES)
U.S. Army Engineer Research and Development Center (ERDC)
Construction Engineering Research Laboratory (CERL)
P.O. Box 9005
Champaign, IL 61826-9005

8. PERFORMING ORGANIZATION REPORT NUMBER
ERDC/CERL TR-01-36

9. SPONSORING / MONITORING AGENCY NAME(S) AND ADDRESS(ES)
Commander, USAADACAFB
Directorate of Environment
Bldg 624, Pleasanton Rd
Fort Bliss, TX 79916-6812

10. SPONSOR/MONITOR'S ACRONYM(S)
ATZC-DOE-C

11. SPONSOR/MONITOR'S REPORT NUMBER(S)

12. DISTRIBUTION / AVAILABILITY STATEMENT
Approved for public release; distribution is unlimited.

13. SUPPLEMENTARY NOTES
Copies are available from the National Technical Information Service, 5285 Port Royal Road, Springfield, VA 22161.

14. ABSTRACT

Fort Bliss, Texas, is a Training and Doctrine Command installation located in the semi-arid Northern Chihuahuan Desert of Western Texas and South Central New Mexico. Military training (both tracked and wheeled vehicles), grazing, and recreational activities act as stressors on the landscape. The natural resource managers need information on land condition to make informed land management decisions and to support conservation and compliance efforts. They need a cost-effective method of assessing and monitoring land condition.

The objective of this research was to characterize the small scale, gross level change in land condition on a selected area of Fort Bliss over a 23-year period. The evaluation and analysis was based on several vegetation and brightness indices calculated from temporal, archival multispectral imagery.

Trends in brightness and greenness indices varied considerably. Most variation could be due to natural differences in the amount of precipitation in the region. There was no indication of permanent, long-term changes in the land condition. The study area appeared to be resilient, with no clearly observable trends in either long-term degradation or improvement. The brightness and greenness indices calculated from temporal image data sets provides a cost-effective method for monitoring relative trends in land condition.

15. SUBJECT TERMS
Ft. Bliss, TX; natural resource management; vegetation; remote sensing; Land Condition Trend Analysis (LCTA); digital imagery

16. SECURITY CLASSIFICATION OF:			17. LIMITATION OF ABSTRACT	18. NUMBER OF PAGES	19a. NAME OF RESPONSIBLE PERSON
a. REPORT	b. ABSTRACT	c. THIS PAGE			Scott Tweddale
Unclassified	Unclassified	Unclassified	SAR	70	19b. TELEPHONE NUMBER (include area code) (217) 352-6511, ext 7409